From the Department of Physics, Lund University

With 9 figures.

Received: July, 17th, 1937

On the Evaporation of Falling Drops

Author
Nils Frössling
Lund (Sweden)

Gerlands Beiträge zur Geophysik (1938) 52, 170-216

Contents

List of Symbols

A, a	Constants (to be determined)
B, b	Constants (to be determined)
B	Atmospheric pressure
c	Concentration (of vapor)
c'	Concentration (of vapor) in undisturbed air
c_m	$= \frac{\mathscr{M}\, p}{\mathscr{R}\, T}$
c_p	Specific heat at constant pressure
D	Diameter of drop $= 2r_0$
$\mathscr{D}$	Diffusion coefficient
f	Wind factor
F	Surface area
h	Convective heat transfer coefficient
L	Characteristic length, e.g. D
m	droplet mass, evaporating mass
$\mathscr{M}$	Molar mass
n	Exponent
n	Normal to the boundary surface parallel to the radius vector r from the origin to the surface in the domain of a sphere centered at its origin
Nu	NUSSELT number $= \frac{\text{Convective heat transfer}}{\text{Conductive heat transfer}} = \frac{hL}{\lambda}$
p	Pressure
p_0	Partial pressure of the vapor
p_m	Saturation pressure
p'	Pressure in undisturbed air
r	radius vector
r_0	droplet radius, radius of the sphere
Re	REYNOLDS number $= \frac{\rho U D}{\eta}$
$\mathscr{R}$	gas constant

t	Time
T	Temperature
u, v, w	Velocity components in x, y and z direction
U	wind speed, relative velocity
v	velocity
x, y, z	Cartesian coordinates
η	dynamic viscosity
θ	Angle between radius vector and polar axis based on a sphere
λ	Thermal conductivity
ν	kinematic viscosity $= \frac{\eta}{\rho}$
ρ	Density
ρ_1	Density of droplet
σ	Constant $= \frac{\mathscr{D}}{\nu}$, in modern notation the reciprocal of the SCHMIDT number
τ	Time interval, evaporation time, oscillation time

Abstract

A theoretical and experimental investigation of the evaporation of a falling drop was made. The drop was put on a thin glass rod or a thermoelement, and an air-current from a wind-tunnel was blown from below. The evaporation was measured by photographing the drop repeatedly on increased scale. The radius of the drop was 0.1 mm to 0.9 mm, the wind velocity 0.2 $\mathrm{m\,s^{-1}}$ to 7 $\mathrm{m\,s^{-1}}$ and the Reynolds number 2-800. Examined liquids: Nitrobenzene, aniline and water. From the measurements the following formula was obtained in agreement with the theory:

$$\frac{\mathrm{d}m}{\mathrm{d}t} = 4\pi\,\mathscr{D}\cdot\frac{\mathscr{M}\,p}{\mathscr{R}\,T}\cdot r\cdot\left(1+k\cdot\sqrt{\mathrm{Re}}\right)\,.$$

$\frac{\mathrm{d}m}{\mathrm{d}t}$ = evaporation in $\mathrm{g\,s^{-1}}$; $\mathscr{D}$ = diffusion constant in $\mathrm{cm^2\,s^{-1}}$; $\mathscr{M}$ = molecule weight; $\mathscr{R}$ = the universal gas constant; T = absolute temperature; p = difference between the pressures of vapor at the surface (approximately the saturation pressure) and in the streaming air; r = radius of the drop; Re = Reynolds number = $\frac{\rho U 2r}{\eta}$; ρ = air density; η = air viscosity; U = relative velocity; (all quantities in CGS). k is a constant characteristic for the evaporating substance that only depends on $\sigma = \frac{\mathscr{D}}{\nu}$. ($\nu$ = kinematic viscosity = $\frac{\eta}{\rho}$). At least approximately

$$k = \frac{0.276}{\sqrt[3]{\sigma}}\,.$$

For the evaporation of naphthalene spheres the same result was obtained. The fluid-drops could therefore, in the examined range, be treated as solid spheres. At naphthalene the evaporation in different zones could be measured. The results of these measurements agree well with those receivable qualitatively from the stream shape.

1 Introduction

The evaporation rate of a drop that is at rest in relation to the surrounding medium has been treated both theoretically and experimentally by the works of Sresnewsky ([46]), Morse ([30]), Smoluchowski ([45]), Jeffreys ([21]), Langmuir ([25]), Gudris and Kulikowa ([18]), Topley and Whytlaw-Gray ([52]), Houghton ([19]), Fuchs ([17]) and others. For stationary conditions and substances that are not particularly volatile, the following formula applies:

$$\frac{\mathrm{d}m}{\mathrm{d}t} = 4\pi \cdot \mathscr{D} \cdot \frac{\mathscr{M}\, p}{\mathscr{R}\, T} \cdot r\,. \tag{1.1}$$

(Designations as in the summary, D = diameter.)
However, the much more complicated problem of evaporation of drops moving relative to the surrounding medium, as in the case of a falling drop, has received very little attention. Fuchs ([17]) showed that at very small Reynolds numbers ($\ll 1$) the total evaporation is equal to that at rest. After designing the present study, I became known to an experimental work by Takahasi ([50], [51]) on the evaporation of water drops with a radius of 0.2 mm to 1 mm and at speeds of $1\,\mathrm{m\,s^{-1}}$ to $6\,\mathrm{m\,s^{-1}}$. His formula, which partially contradicts my theoretical and experimental results, is discussed at the end of this paper. An investigation of this problem is also of great interest for meteorological questions (applicability to raindrops), for the theory of evaporation in general (testing of similarity- and boundary layer-theories; possibility of an experimental investigation of the mathematically very difficult to treat Re-range between those at large and small friction and for the theory of heat transfer (which is analogous to that of evaporation)). The evaporation is greater when the object is moving than when resting. According to Equation 1.1 one can make the following approach:

$$\frac{\mathrm{d}m}{\mathrm{d}t} = 4\pi r \cdot \mathscr{D} \cdot \frac{\mathscr{M}\, p}{\mathscr{R}\, T} \cdot f\,. \tag{1.2}$$

f is hereinafter referred to as the wind factor; It indicates the multiple by which evaporation has increased as a result of the movement. The aim of this study was primarily to theoretically and experimentally determine the dependence of the wind factor on the droplet size, speed and material constants. In addition, the distribution of evaporation over the droplet surface was measured. Since the non-stationary problem is extremely complicated, only the stationary one was treated. Constant values for speed and evaporation are therefore assumed over time.

2 Theoretical Part

2.1 General Remarks

For now, the drops are treated as solid and spherical. (The applicability of this requirement will be discussed later). Evaporation occurs when the molecules leave the drop surface and continue to diffuse through the air. Since this diffusion usually occurs much more slowly than the vapor formation at the interface, stagnation occurs at the interface. During their irregular movements, many molecules hit the drop surface again and are partly absorbed by it. Therefore, a condensation of molecules also occurs. A state of equilibrium soon occurs between evaporation, diffusion and condensation. The vapor is then almost saturated at the surface of the drop (the deviation will be calculated later). If one introduces the saturation pressure as a boundary condition, one can treat evaporation as a pure diffusion problem. Stefan ([47], [48] [49]) was probably the first to recognize this. To solve the problem one first makes use of the Navier-Stokes equation, the continuity equation and the boundary conditions of the flow in order to be able to calculate the velocity field. The concentration field is obtained from the equation for diffusion in a moving medium (e.g. according to Jeffreys [21]) and from the boundary conditions of the vapor. Evaporation is then calculated from the concentration gradient at the surface. In a rectangular coordinate system (x, y, z) at rest relative to the body, the velocity components are u, v, w, the pressure is P and the concentration is c. If compressibility and the force due to gravity are neglected, we get:

$$\left.\begin{aligned} u\frac{\partial u}{\partial x}+v\frac{\partial u}{\partial y}+w\frac{\partial u}{\partial z} &= -\frac{1}{\rho}\cdot\frac{\partial P}{\partial x}+\frac{\eta}{\rho}\cdot\left(\frac{\partial^2 u}{\partial x^2}+\frac{\partial^2 u}{\partial y^2}+\frac{\partial^2 u}{\partial z^2}\right), \\ u\frac{\partial v}{\partial x}+v\frac{\partial v}{\partial y}+w\frac{\partial v}{\partial z} &= -\frac{1}{\rho}\cdot\frac{\partial P}{\partial y}+\frac{\eta}{\rho}\cdot\left(\frac{\partial^2 v}{\partial x^2}+\frac{\partial^2 v}{\partial y^2}+\frac{\partial^2 v}{\partial z^2}\right), \\ u\frac{\partial w}{\partial x}+v\frac{\partial w}{\partial y}+w\frac{\partial w}{\partial z} &= -\frac{1}{\rho}\cdot\frac{\partial P}{\partial z}+\frac{\eta}{\rho}\cdot\left(\frac{\partial^2 w}{\partial x^2}+\frac{\partial^2 w}{\partial y^2}+\frac{\partial^2 w}{\partial z^2}\right), \end{aligned}\right\} \tag{2.1}$$

$$\frac{\partial u}{\partial x}+\frac{\partial v}{\partial y}+\frac{\partial w}{\partial z}=0\,, \tag{2.2}$$

$$u\frac{\partial c}{\partial x}+v\frac{\partial c}{\partial y}+w\frac{\partial c}{\partial z}=\mathscr{D}\cdot\left(\frac{\partial^2 c}{\partial x^2}+\frac{\partial^2 c}{\partial y^2}+\frac{\partial^2 c}{\partial z^2}\right). \tag{2.3}$$

For large x and y or z $u = U$; $v = w = 0$; $c = 0$ applies.
For $x^2 + y^2 + z^2 = \frac{D^2}{4}$ $u = v = w = 0$; $c = c_m$ applies.

$$\frac{\mathrm{d}m}{\mathrm{d}t} = -\mathscr{D} \cdot \int_{(F)} \left(\frac{\partial c}{\partial n}\right)_{\text{Ob.}} \mathrm{d}F\,; \tag{2.4}$$

When it comes to heat transfer, an analogous system is obtained. There is no known method for the exact solution of such systems. But by converting them into dimensionless form one can make certain similarity considerations. The first to treat similarity in temperature and concentration fields was Nusselt ([32], [33]). If one introduces the dimensionless quantities x_1, y_1, z_1 etc. into the above equations with the following substitutions:

$$\begin{array}{lll} x = x_1 \cdot D & u = u_1 \cdot U & P = P_1 \cdot U^2 \rho \\ y = y_1 \cdot D & v = v_1 \cdot U & c = c_1 \cdot c_m \\ z = z_1 \cdot D & w = w_1 \cdot U & F = F_1 \cdot D^2 \\ n = n_1 \cdot D & & \end{array}$$

and

$$\frac{\rho U D}{\eta} = \mathrm{Re}\,; \quad \frac{\mathscr{D}}{UD} = \frac{\sigma}{\mathrm{Re}}\,,$$

Equation 2.1, Equation 2.2 and Equation 2.3 and the boundary conditions only contain Re and σ apart from the indexed quantities. Equation 2.4 yields

$$\frac{\mathrm{d}m}{\mathrm{d}t} = -\mathscr{D}\, c_m D \cdot \int_{(F_1)} \left(\frac{\partial c_1}{\partial n_1}\right)_{\text{Ob.}} \mathrm{d}F_1\,. \tag{2.5}$$

The quantities u_1, v_1, w_1 and P_1 therefore become functions of Re, x_1, y_1, z_1. Then, from the diffusion equation one obtains

$$c_1 = \text{function } (\mathrm{Re}, \sigma, x_1, y_1, z_1)\,.$$

Introducing this expression in Equation 2.5 gives[1], when $c_m = \frac{\mathscr{M}\, p}{\mathscr{R}\, T}$

$$\frac{\mathrm{d}m}{\mathrm{d}t} = -\mathscr{D} \cdot \frac{\mathscr{M}\, p}{\mathscr{R}\, T} \cdot D \cdot \text{function } (\mathrm{Re}, \sigma)\,.$$

Comparing this expression with Equation 1.2 one obtains

$$f = \text{function } (\mathrm{Re}, \sigma)\,. \tag{2.6}$$

For given materials, the wind factor f therefore only depends on Re.

[1] If, as in the water experiments, the pressure of the vapor in the undisturbed air does not equal 0; but is equal to p', then $p = p_m - p'$.

2.2 The Form of the Function f

A solution is only possible for very small or very large Reynolds numbers. For $\mathrm{Re} \ll 1$ the evaporation will become according to FUCHS, as stated above, the same as that in quiescence, so $f = 1$.
For $\mathrm{Re} \gg 1$ one can derive important conclusions via the boundary layer theory of PRANDTL ([38]). According to this theory at large Re numbers the effect of friction is only present in a thin layer near the surface of the body. In this layer the velocity grows very fast beginning from zero, whereas in the outer region there prevails a potential flow.

The pressure in this layer is independent from the distance to the wall at a given stagnation point distance and equals that of the potential flow near outside the layer.

As the theory demands, the boundary layer separates from the surface at a certain point (separation point) and a keel-"water" subject to rotation emerges. If one knows the pressure distribution outside the boundary layer, one can calculate the velocity distribution within it and the position of the separation point. One can either use an experimentally determined pressure distribution or calculate the potential flow according to the OSEEN-ZEILON asymptotic theory with a known wake shape.
The nature of the boundary layer is decisive for evaporation because the innermost part is almost stationary and the vapor is almost saturated here. Since the vapor is quickly carried away from the external region, a thin vapor boundary layer is created in which the concentration decreases from almost complete saturation to the value of the external air. During heat transfer, an analogous temperature boundary layer is created. For the boundary layers, if one omits terms of smaller order, Equation 2.1 to Equation 2.3 become simpler.
BOLTZE ([11]) established the equation for the velocity boundary layer for rotating bodies whose axis lies in the direction of the flow. Equation 2.1 to Equation 2.2, which refer to a rectangular coordinate system, are converted to a new one in which y is the length of the normal to the surface and x is the length of the meridian curve from the stagnation point to the base point of the normal. The velocity components parallel and perpendicular to the wall are called u and v. $\overline{u}$ is the speed of the potential flow at the edge of the boundary layer. BOLTZE calculated for the steady state:

$$u\frac{\partial u}{\partial x} + v\frac{\partial u}{\partial y} = \overline{u}\frac{\partial \overline{u}}{\partial x} + \frac{\eta}{\rho} \cdot \frac{\partial^2 u}{\partial y^2}$$
$$\frac{\partial (r'u)}{\partial x} + \frac{\partial (r'v)}{\partial y} = 0\,,$$

where $r' = \perp$ is the distance from the rotational axis.

The equations for temperature and vapor boundary layers have already been established for two-dimensional flows ([39]). Since this is probably missing for the three-dimensional case, the equation for the sphere is derived here. Equation Equation 2.3 appears in vector form (v = velocity vector):

$$(v, \operatorname{grad} c) = \mathscr{D} \cdot \operatorname{div} \operatorname{grad} c \,. \tag{2.7}$$

In a polar system with the pole at the center of the sphere and the polar axis opposite to the direction of flow, let r be the radius vector and θ the angle between the former and the polar axis. Because of the rotational symmetry, the diffusion equation in this system reads:

$$\frac{u}{r} \cdot \frac{\partial c}{\partial \theta} + v \frac{\partial c}{\partial r} = \mathscr{D} \cdot \left[\frac{1}{r^2} \frac{\partial}{\partial r} \left(r^2 \cdot \frac{\partial c}{\partial r} \right) + \frac{1}{r^2 \cdot \sin(\theta)} \cdot \frac{\partial}{\partial \theta} \left(\sin(\theta) \cdot \frac{\partial c}{\partial \theta} \right) \right] .$$

Here, the value for $r = r_0 + y$ and $x = r_0 \cdot \theta$, where r_0 is the radius of the sphere; For a thin layer ($y \ll r_0$) one obtains

$$u \frac{\partial c}{\partial x} + v \frac{\partial c}{\partial y} = \mathscr{D} \cdot \left(\frac{\partial^2 c}{\partial y^2} + \frac{2}{r_0} \cdot \frac{\partial c}{\partial y} + \frac{\partial^2 c}{\partial x^2} + \frac{1}{r_0} \cdot \frac{\partial c}{\partial x} \cdot \cot \left(\frac{x}{r_0} \right) \right) .$$

If the magnitude of the boundary layer thickness is ϵ, that of the radius is 1 and

$$\cot \left(\frac{x}{r_0} \right) \ll \frac{1}{\epsilon^2} \,,$$

the final boundary layer equation is obtained for $\epsilon \ll 1$ as:

$$u \frac{\partial c}{\partial x} + v \frac{\partial c}{\partial y} = \mathscr{D} \cdot \frac{\partial^2 c}{\partial y^2} \,. \tag{2.8}$$

The condition

$$\cot \left(\frac{x}{r_0} \right) \ll \frac{1}{\epsilon^2}$$

is equivalent to

$$\frac{x}{r_0} \gg \epsilon^2 \,.$$

Equation 2.8 therefore applies to all points that are not very close to the stagnation

point. So for the boundary layer we have:

$$u\frac{\partial u}{\partial x} + v\frac{\partial u}{\partial y} = \overline{u}\frac{\partial \overline{u}}{\partial x} + \frac{\eta}{\rho}\cdot\frac{\partial^2 u}{\partial y^2}$$

$$\frac{\partial u}{\partial x} + \frac{\partial v}{\partial y} + \frac{u}{r_0}\cdot\cot\left(\frac{x}{r_0}\right) = 0$$

$$u\frac{\partial c}{\partial x} + v\frac{\partial c}{\partial y} = \mathscr{D}\cdot\frac{\partial^2 c}{\partial y^2}$$

$$\begin{aligned} y = 0 \qquad & y = \text{large} \\ u = v = 0 \qquad & u = \overline{u} \\ c = c_m \qquad & c = 0\,. \end{aligned}$$

The second equation of this system was obtained from Boltze's continuity equation. We now make the following substitutions:

$$\begin{aligned} x &= x_1 \cdot D \\ y &= y_1 \cdot \frac{D}{\sqrt{\mathrm{Re}}} \\ u &= u_1 \cdot U \\ v &= v_1 \cdot \frac{U}{\sqrt{\mathrm{Re}}} \\ c &= c_1 \cdot c_m \\ \overline{u} &= \overline{u}_1 \cdot U \end{aligned}$$

as well as

$$u_1\frac{\partial u_1}{\partial x_1} + v_1\frac{\partial u_1}{\partial y_1} = \overline{u}_1\frac{\partial \overline{u}_1}{\partial x_1} + \frac{\partial^2 u_1}{\partial y_1^2}$$

$$\frac{\partial u_1}{\partial x_1} + \frac{\partial v_1}{\partial y_1} + 2u_1\cdot\cot\left(2x_1\right) = 0$$

$$u_1\frac{\partial c_1}{\partial x_1} + v_1\frac{\partial c_1}{\partial y_1} = \sigma\frac{\partial^2 c_1}{\partial y_1^2}$$

$$\begin{aligned} y_1 = 0 \qquad & y_1 = \text{large} \\ u_1 = v_1 = 0 \qquad & u_1 = \overline{u}_1 \\ c_1 = 1 \qquad & c_1 = 0\,. \end{aligned}$$

The following can be said about the term $\overline{u}_1\frac{\partial \overline{u}_1}{\partial x_1}$: If Re is so large that the square law of resistance applies, experience shows that the wake in subcritical flow has a shape that is almost independent of Re (e.g. Luthander and Ryberg ([26])). This results in a constant pressure distribution, which has been confirmed by

measurements (KRELL ([22])). It further follows that $\overline{u}_1 \frac{\partial \overline{u}_1}{\partial x_1}$ must be the same function of x_1 for all large Re numbers. The same applies to $\overline{u}_1$.
Since the system of equations for the indexed quantities does not contain Re, u_1 and v_1 are only functions of x_1 and y_1. At the separation point, $\frac{\partial u_1}{\partial y_1}$ for $y_1 = 0$ holds good. The position of this point is therefore independent of Re (given the initial profile). This was at least approximately confirmed experimentally (LUTHANDER and RYBERG ([27])). The separation point fluctuates a little, but the middle position follows a circular line (FLACHSBART ([15])). For these, θ_α is approximately equal to 80°. We now calculate the evaporation in front of the separation circle. Since u_1 and v_1 were only functions of x_1 and y_1, it follows that $c_1 = f(x_1, y_1, \sigma)$. If we move on to the dimensioned quantities c, x and y, we get

$$\frac{c}{c_m} = \Phi\left(\frac{x}{D}, \frac{y\sqrt{\mathrm{Re}}}{D}, \sigma\right).$$

The evaporation through the boundary layer is

$$\begin{aligned}\frac{\mathrm{d}m}{\mathrm{d}t} &= -\mathscr{D} \cdot \int \left(\frac{\partial c}{\partial y}\right)_{y=0} \mathrm{d}F \\ &= -\mathscr{D}\, c_m \cdot \int_0^{\theta_\alpha} \left[\frac{\partial}{\partial y}\Phi\left(\frac{x}{D}, \frac{y\sqrt{\mathrm{Re}}}{D}, \sigma\right)\right]_{y=0} \cdot \frac{\pi D^2}{2} \cdot \sin(\theta)\,\mathrm{d}\theta\,;\end{aligned}$$

$$\left(\frac{\partial \Phi}{\partial y}\right)_{y=0} = \frac{\sqrt{\mathrm{Re}}}{D} \cdot \left[\frac{\partial}{\partial y}\Phi\left(\frac{x}{D}, \psi, \sigma\right)\right]_{\psi=0} = \frac{\sqrt{\mathrm{Re}}}{D} \cdot \Phi_1\left(\frac{x}{D}, \sigma\right)\ ;\ \frac{x}{D} = \frac{\theta}{2}\,;$$

$$\therefore \frac{\mathrm{d}m}{\mathrm{d}t} = -\mathscr{D}\, c_m \cdot \sqrt{\mathrm{Re}} \cdot D \cdot \int_0^{\theta_\alpha} \frac{\pi}{2}\Phi\left(\frac{\theta}{2}, \sigma\right) \sin(\theta)\,\mathrm{d}\theta\,.$$

Since the integral is just a function of σ, we get

$$\frac{\mathrm{d}m}{\mathrm{d}t} = 4\pi \cdot \mathscr{D} \cdot \frac{\mathscr{M}\, p}{\mathscr{R}\, T} \cdot r_0 \cdot k(\sigma) \cdot \sqrt{\mathrm{Re}}\,. \tag{2.9}$$

This is just the evaporation before the circle of separation. Calculations are very difficult in the wake because of the irregular vortex movement. However, the movement in the wake is quite slow ([40]). One can therefore expect that evaporation here is quite low. This was also confirmed by my own measurements on naphthalene spheres. For Re = 700 and 1000, the evaporation on the front half of the sphere was 75 % to 80 % of the total. If the evaporation on the rear side, which grows with Re, is set approximately proportional to $\sqrt{\mathrm{Re}}$, the total evaporation will not be affected by any major error. One can therefore use Equation 2.9 also for the total evaporation of the sphere. Only the numerical value for k is changed

slightly. By comparing with Equation 1.2 we get for large Re numbers:

$$f = k \cdot \sqrt{\mathrm{Re}}\,.$$

This formula was derived without the need to know the distribution of velocity and concentration in the boundary layer. However, this may be necessary when calculating the function $k(\sigma)$. However, without carrying out these more complicated calculations, one can say that k decreases as σ increases. Then the vapor boundary layer becomes thicker because the vapor diffuses further outwards before it is carried away by the flow. The distance along which c falls from c_m to 0 becomes longer. The evaporation rate of a substance with a large diffusion constant is therefore relatively little influenced by the wind. For the two-dimensional case, the heat transfer was calculated for two bodies: by Pohlhausen ([35]) for a flat plate parallel to the flow and by Kroujiline ([24], [23]) for a circular cylinder. The size σ corresponds to the number $\frac{\lambda}{\nu c_p \rho}$ when heat is transferred. (λ = thermal conductivity; c_p = specific heat at constant pressure). According to the calculations mentioned, which also apply to evaporation, at large Re numbers the transition for the circular cylinder and the plate is directly proportional to the quantity $\sqrt{\mathrm{Re}}$ and inversely proportional to $\sqrt[3]{\sigma}$. Although it is not permitted to transfer the latter result to the sphere, one can try the approach

$$k = \frac{\text{const.}}{\sigma^n} \tag{2.10}$$

when determining k experimentally. In this case, although not necessarily, n is probably close to $\frac{1}{3}$. The above-mentioned determinations for the boundary layer only apply under the condition that the boundary layer for the vapor is not significantly thicker than that for the velocity. For the plate and the cylinder, both quantities were equal for $\sigma = 1$ and 0.39, respectively; So σ cannot be significantly larger than 1 here. For the substances examined, $\sigma = 1.7$ for water and for the other substances σ was less than 1.
Proportionality between evaporation and $\sqrt{\mathrm{Re}}$ at large Re numbers was previously empirically determined for porous spheres (Büttner ([12])).

Summary of the theoretically obtained results that shall be tested by the experiment and the questions that are intended to be answered by the results of the experiments:

1. f = funct.(Re) for every substance and is large for substances with small $\mathscr{D}$. The same f should therefore be obtained for different drop sizes with common Re numbers.

2. The form of this function is to be determined experimentally. One can expect that at small Re $f = 1$ and at large Re $f = k \cdot \sqrt{\mathrm{Re}}$.

3. If the latter holds, k must decrease as σ increases. The function $k(\sigma)$ is to be determined experimentally and is approximately $k = \frac{\text{const.}}{\sigma^n}$, where n is probably close to $\frac{1}{3}$.

4. The distribution of evaporation over the surface is to be investigated.

3 Experimental Part

3.1 Experimental Arrangements and Measurement Methods

3.1.1 General Remarks

An accurate, direct measurement of evaporation during the fall of a drop may not be possible. Since all that matters is the relative speed between the drop and the air, the same evaporation and therefore the same results are obtained if the drop is kept at rest and exposed to a wind of the corresponding speed. During the experiments, the drops were suspended from a thin glass thread or a thermocouple and blown at them with the airflow from a wind tunnel. The evaporation rate was measured by repeated photography. Figure 3.1 shows the experimental setup.

3.1.2 The Suspension of the Evaporating Materials

The semi-volatile liquids nitrobenzene and aniline were examined, in which the cooling was small due to evaporation, and water, in which the temperature dropped significantly. In the first case, the drop was suspended on a glass thread (diameter 0.02 mm to 0.2 mm). To ensure that this thread remained in place, a glass rod was drawn to a very thin tip and the other end was cemented into a metal tube. The tube could then be clamped in a tripod without vibration. In order to avoid the great uncertainty of a temperature calculation, the water drops were placed on a thermocouple made of thin constantan and manganine wires (diameter 0.05 mm and 0.1 mm, respectively) and the drop temperature was thereby measured directly. To achieve a stable suspension, insulated wires were passed through a drawn glass tube and sealed at the entry point. Manganin was used instead of the usual copper because its thermal conductivity is only about one-twentieth that of copper and therefore the droplet temperature is less affected, while the "thermoforce" is almost the same. The drops were prepared using thin pipettes. In order to compare the evaporation of liquid drops with that of a solid sphere and to measure the distribution of evaporation over the surface, the evaporation of a solid substance was also examined. To do this, a little of this material was melted onto a glass thread to form a drop, which was then allowed to solidify. Several substances of suitable volatility were tested, but most could not be used because they crystallized upon solidification. Finally, sufficiently good spheres were obtained from naphthalene by

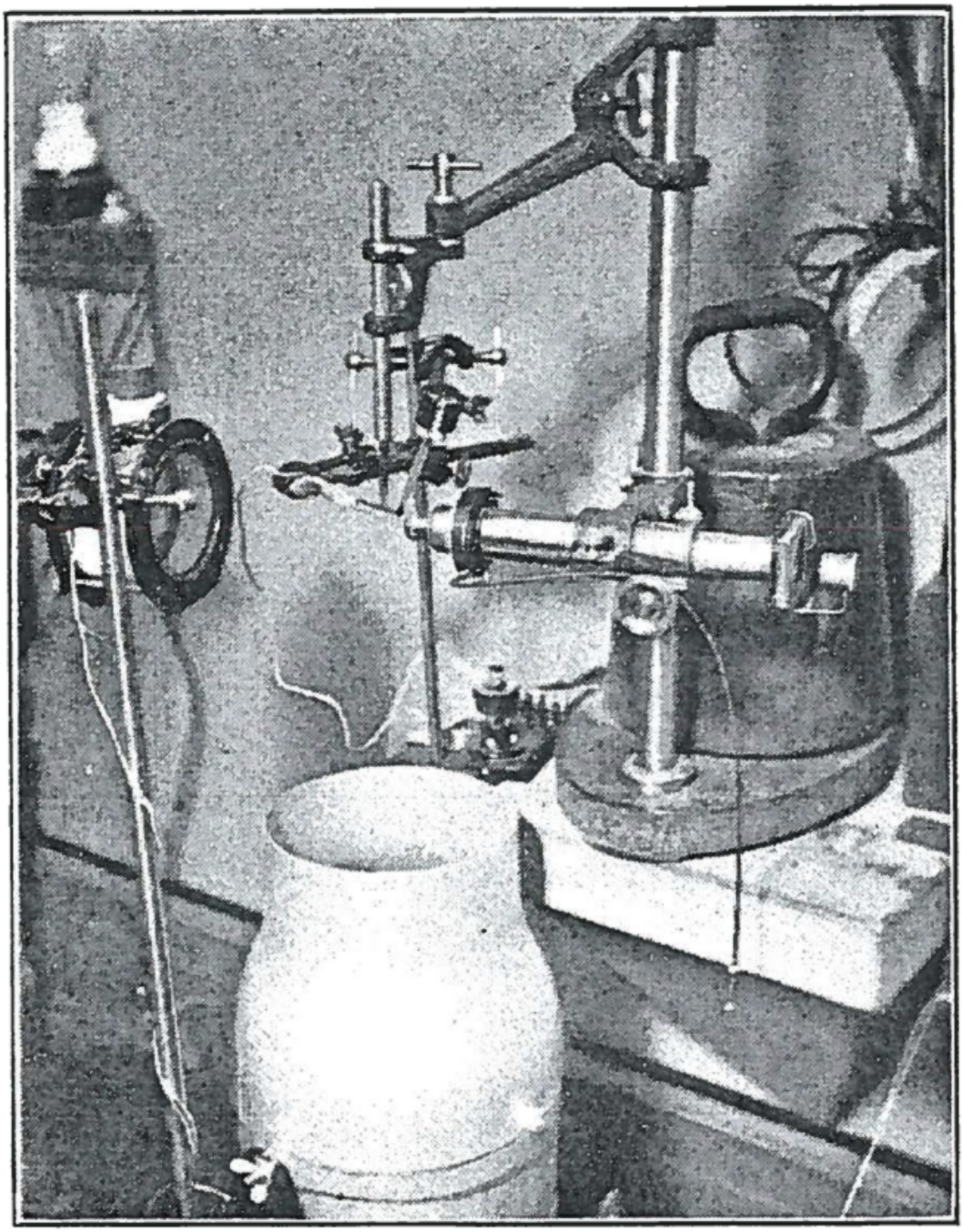

Figure 3.1: Experimental setup for measuring evaporation of falling drops

repeatedly gently heating the solidified sphere so that the outer parts melted and then rapidly cooling it. The glass thread, which was quite coarse to avoid bending by the wind, was bent at right angles near the sphere. The sphere was turned towards the camera so that its equatorial section was photographed. This had two advantages. In some cases a well circular image was obtained, in other cases all points on the line to be photographed had the same temperature when heated, which is why any possible chemical transformation could not have any influence on the distribution curve.

3.1.3 The Photographic Recording

The drops were photographed at approximately seven times magnification. A microscope lens was used as the objective. The image distance (approx. 16 mm) was chosen for the camera length used so that, on the one hand, it was not so small that the air flows were disturbed at the drop, and on the other hand, it was not so large that the aperture became too small to provide the necessary sharpness on the plate. The fact that the above-mentioned malfunction did not occur was determined by smoke tests. The camera length was variable to maintain focus. The dependence of magnification on length was determined by photographing an object micrometer. The parallax error in the photographic determinations of droplet evaporation was calculated to be <0.5 %. For the reliability of the results, it was particularly important that the distance between the drop and the camera during evaporation was fixed. For this purpose, the mounting for the drops and the camera were clamped to a common, strong tripod that was protected from the vibrations of the wind tunnel. Furthermore, it was calculated that a shift so large that the result would be falsified due to the change in magnification would have to cause significant blurring on the plate. The Agfa contrast plates proved to be a suitable plate material. The drops were imaged two to four times on the same plate. This avoided any possible displacements when changing plates, and it was possible to adjust the measurement, which was done with a comparator, to exactly corresponding points on the edge of the drop. A very precise measurement was necessary because the evaporation was to be measured for different drop sizes and the diameter was therefore only allowed to decrease by around 10 % during the experiments. This small reduction should then, if possible, be measured to the nearest 1 %. A drop with a diameter of 1 mm had to be measured to 0.001 mm. The fact that this was achieved was shown by the fact that various comparator settings for the diameter resulted in values that usually only deviated by around 0.5 µm from the mean value. Another advantage of exposing the same plate multiple times was that the evaporation distribution of naphthalene could be monitored. A 4.5 V light bulb was used to illuminate the drops. To turn off the thermal radiation from this lamp, a container containing copper sulfate solution was placed in front of the lamp. During the exposure, which lasted 1 to 3 seconds, the air flow was switched off by inserting a plate to avoid the weak trembling of the drops. Figure 3.2 shows some of the photographs. Figure 3.2-1 to Figure 3.2-3 on an enlarged scale.

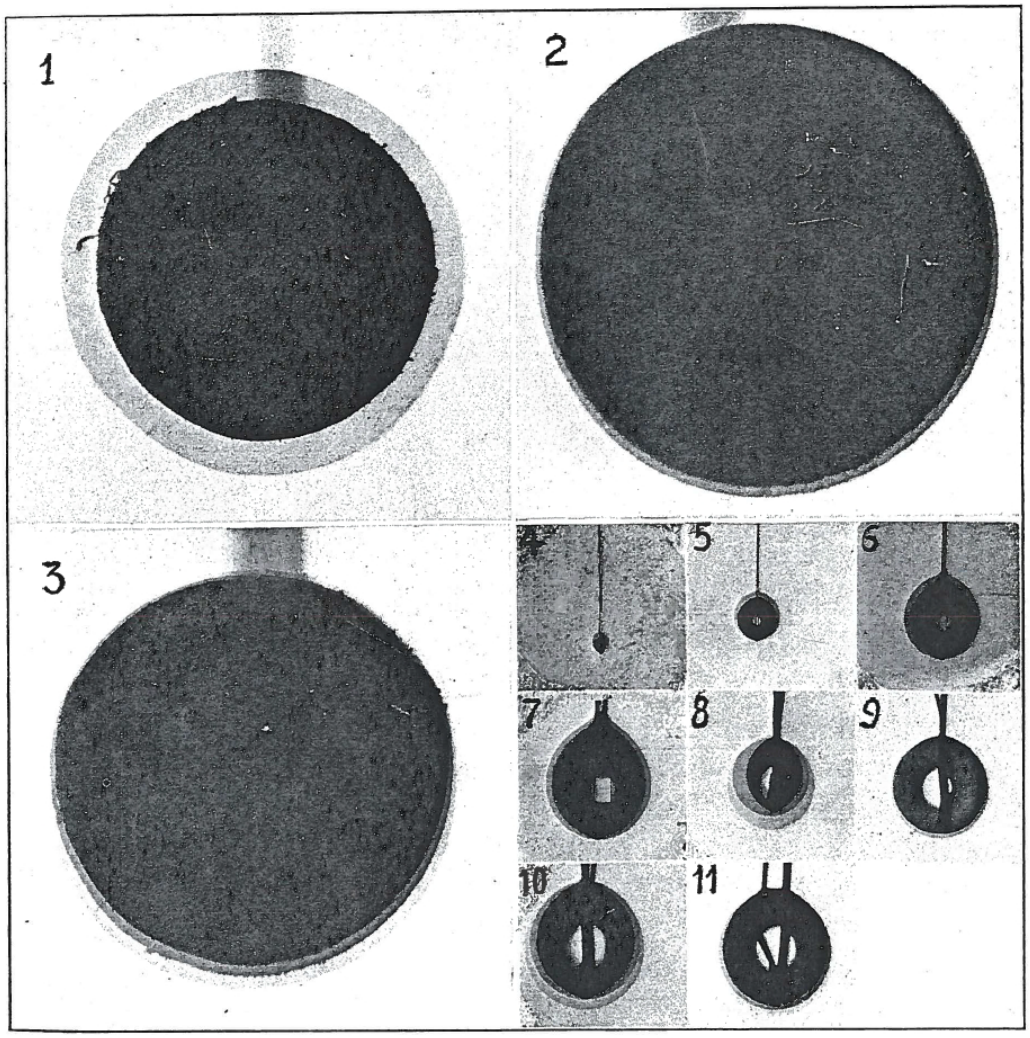

Figure 3.2: 1–3 naphthalene; 4–7 nitrobenzene; 8–11 water

3.1.4 The Wind Tunnel

A wind tunnel according to Roller ([37]) was used to generate the air flow. Since the channel is described in detail in the location cited, little is reported here. The channel, which can be adjusted in any direction, was directed so that the flow hit the drops from below. This was beneficial for several reasons. When the drop is blown from the side, it shifts in the direction of the wind, and the glass thread in this case causes a considerable disturbance on the front side of the drop. When blowing from below, the deformations will be small due to gravity. In addition, speed pulses that arise from the temperature difference between the jet and the external air cannot act perpendicular to the stream as with a horizontal flow, which would be particularly disruptive at low wind speeds. The drops were placed 20 cm above the outlet of the wind tunnel. Nozzles with 10, 16 and 20 cm orifice diameters were used in the experiments. The turbulence, as determined through experiments, was not great, particularly when the smallest nozzle opening was used. The smoke from a cigarette in the wind tunnel rose from the outlet in narrow, almost straight lines. The information about the wind force distribution in the above paper was checked, and in accordance with this, a change in air velocity in the flow direction of $<1\,\%$ for 15 cm, and perpendicular to it of $<1\,\%$ for 1 cm, was found at the location of the drop. Since the diameter of the examined objects was less than 2 mm, the wind tunnel was well suited for this investigation. The motor was fed with direct current under potentiometer switching. The velocity range used was $0.2\,\mathrm{m\,s^{-1}}$ to $7\,\mathrm{m\,s^{-1}}$ for drops and $0.2\,\mathrm{m\,s^{-1}}$ to $12\,\mathrm{m\,s^{-1}}$ for naphthalene spheres. At low wind speeds, battery voltage was used instead of mains voltage.

3.1.5 Measuring Wind Speed

Wind speed should be measured to the nearest 1 % if possible. Because the cross-section of the jet was quite small, it was necessary to use a measuring device that provided the average velocity in a very small area and was small enough not to disturb the flow. One also had to be able to read the instantaneous values in order to be able to keep the speeds constant by regulating them. Therefore, cup cross or vane anemometers were inapplicable. For speeds over $2\,\mathrm{m\,s^{-1}}$ a PRANDTL pitot tube was used and for smaller speeds a hot wire anemometer was used. The pitot tube, whose diameter was 1 cm, was placed 2 cm from the drop, so that the flow was not disturbed (after smoke tests). The small change in the measured values when moving the pipe to the location of the drop was determined for different speeds, and the wind strength values read were corrected accordingly in the evaporation tests. The micromanometer was filled with alcohol and had two vertical legs with very different cross-sections. The pressure could therefore be observed by applying a small correction factor due to the fluctuations of the liquid in the thinner tube. For wind speeds $<7.5\,\mathrm{m\,s^{-1}}$, a reading microscope with a large image distance was used and for larger ones, a cathetometer was used. In the first case, the parallax

error was calculated to be less than 3 ‰, and in fact the information from the microscope and the cathetometer agreed well with large deflections. An ALBRECHT hot-wire anemometer ([6]) was used with the introduction of various improvements. The two platinum wires, connected in the same way in a bridge arrangement, had a length of 1 cm and a diameter of 15 and 30 µm. They were soldered parallel to three copper wires mounted on a rod at a distance of 2 mm. This arrangement hardly disturbed the flow through the measuring device. The sensitivity of the galvanometer could be reduced with a shunt. The manganin balancing resistors (approx. 10 and 40 Ω) were adjusted so that the galvanometer (with high sensitivity) was de-energized when the current was so small that heating could be neglected (1 mA). The corner points of the bridge circuit were soldered. The lower sensitivity of the galvanometer was used in the measurements. The current (0.1000 A in the outer cable) was supplied by a 30 V battery through a large resistor so that changes in wind strength and therefore in the resistance of the platinum wires should not have a large effect on the current strength. The current strength of 0.1000 A was adjusted when there was no wind. When the platinum wires were heated, the galvanometer gave a deflection (n), which was measured. Since the balance of the bridge gradually changed on its own, n was corrected accordingly. This correction was determined with weak current and high galvanometer sensitivity. In order to eliminate thermal forces, measurements were also carried out with switched current. The anemometer was calibrated using a rotary device. The connection to the galvanometer and to the power source was achieved by brush and slip rings (made of copper to avoid thermal forces). In order to reduce the entrainment of air, the arm of the apparatus had a streamlined cross-section. It was determined by smoke tests that the entrainment was not greater than 1 % in the speed range used (0.2 m s^{-1} to 2.5 m s^{-1}) and could therefore be neglected. Using a formula from King ([41]) one can show that n is proportional to the expression

$$\frac{1}{(1 + a \cdot \sqrt{U})} - \frac{1}{4 \cdot \left(1 + a \cdot \sqrt{2U}\right)} .$$

(a = a constant; U = speed). In the speed range used, this expression can be set inversely proportional to the size $(1 + b \cdot \sqrt{U})$ with an error <1 %. One gets in this way:

$$U = \left(\frac{A}{n} - B\right)^2 . \tag{3.1}$$

Here A and B are constants that need to be determined by calibration. In the $\frac{1}{n}$-$\sqrt{U}$ diagram, the calibration curve must result in a straight line, which actually happens. The deviation of the calculated values from those observed was rarely >1 %. Because of the well-known property of the hot-wire anemometer to change the calibration value over time, the wires were heated for several days with a current of more than 0.1000 A and the calibration was checked often. The humidity

was occasionally monitored so that the calibration fluctuations that occur when humidity changes according to Paeschke ([34]) and Schubauer ([44]) did not falsify the results. The effect of the convection wind, which according to Cooper and Linton ([13], [14]) causes different values at very low speeds depending on whether the wires are vertical or horizontal, can be neglected here based on calculations. During the evaporation tests, the hot wires were placed approximately 7 mm above and 5 mm next to the drops. After control tests, the speed could be set to be the same as that near the drop. That the heated wires did not affect the droplet temperature was shown by hanging the drops on a thermocouple. The Pitot tube and the hot-wire anemometer, at about $2\,\mathrm{m\,s^{-1}}$, where their sensitivity was approximately the same, gave results, when measuring the same air flow, that differed from each other by less than 2 %. In the experiments, the speed values can be safely viewed at around 1 %.

3.1.6 Measuring Temperature

Evaporation is highly dependent on temperature. Since the vapor pressure of the substances examined changed by 5 % to 10 % per degree, the temperature had to be known to an accuracy of around 0.1 °C in order to avoid errors >1 %. An approximately constant temperature (to 0.1 °C to 0.2 °C) was maintained in the room using a thermoregulator. To mix the air in the room, a fan with a low speed was used, which generated a wind of only approx. $1\,\mathrm{cm\,s^{-1}}$ at the experimental site. It was stopped during tests with small wind speeds. The experiments were carried out at 20 °C. The air temperature was measured with a thermocouple (due to small inertia) for nitrobenzene, aniline and naphthalene. As mentioned above, the water drops were hung on a thermocouple, which allowed the droplet temperature to be measured directly. The reason why glass wires were preferred for suspension was that they allowed the study to be extended to much smaller drop sizes. During the experiments, the temperature and speed were read repeatedly and the average values were used. Air pressure was also monitored because of its effect on evaporation. How the temperature and the barometer reading were calculated will be mentioned later.

3.1.7 The Arrangement of the Measurements at no Wind

To calculate the wind factor f, one needs to know not only the evaporation at the speed in question, but also that at no wind, i.e. at stationary conditions. This quantity can be calculated from Equation 1.1, but since no exact values are known for the diffusion constant and the vapor pressure for nitrobenzene, aniline and naphthalene, the evaporation of these substances in the absence of wind must be determined directly. A glass cylinder (length 12 cm, diameter 5 cm) closed at the end was pushed over the front part of the camera. Holes were drilled in the cylinder for the insertion of the drop carrier and the thermocouple. The inner surface

was covered with burnt charcoal to absorb the fumes. It is important that the evaporation really corresponds to Equation 1.1 and is not increased by convection. After smoke tests, the air disturbance could be neglected given the cylinder volume used. Free convection as a result of density changes caused by lower temperatures and partial saturation is difficult to calculate. To do this one would have to find the speed of the external air and from that the evaporation. However, it can be shown by the following arguments that free convection can be neglected for the droplet sizes used, at least for the low-volatility substances nitrobenzene, aniline and naphthalene:

1. In the experiments by Topley and Whytlaw-Gray ([52]), iodine (at which the effect is of the same magnitude) measured an evaporation that agrees well with Equation 1.1. In my experiments, the values for aniline agreed within the error limits with the values that can be calculated from the previously known values for $\mathscr{D}$ and p found in other ways (see below). No precise determinations of $\mathscr{D}$ were available for nitrobenzene and naphthalene.

2. An effect of convection should be greater at large radii. However, in the experiments by Topley and Whytlaw-Gray ([52]) and by me, no such variation in values was obtained.

3. Convection would disrupt the even distribution of evaporation over the surface. Because the convection current is directed downward, evaporation had to be greater on the upper side. This did not happen in my experiments with naphthalene (see below).

The correction due to the limited evaporation space, e.g. according to Fuchs ([17]), was taken into account.

3.1.8 Measurement of the Plates and Calculating Evaporation

The experiments were intended to measure the evaporation $\frac{\mathrm{d}m}{\mathrm{d}t}$ at different diameters D and wind speeds U. To examine evaporation during stationary falling motion, one should actually only use the speed that corresponds to the diameter in question. However, since the average diameter depends on the amount of material evaporated and cannot be known in advance, and further there must also be a certain uncertainty in the calculation of the falling speed, the wind speed was varied within the widest possible limits. This also made it possible to test the laws of similarity. Furthermore, if these were confirmed, one could obtain the evaporation of a drop whose dimensions are outside the experimental limits by using an equivalent speed for a different drop size. During the known time δt the drop loses the measured mass δm and its diameter decreases from D_0 to D_1. $\frac{\delta m}{\delta t}$ was assumed as the value of the average evaporation rate. As the diameter changes during the test, $\frac{\mathrm{d}m}{\mathrm{d}t}$ cycles through a range of different values. However,

the measured average evaporation $\frac{\delta m}{\delta t}$ corresponds (according to the mean value theorem of differential calculus) to the instantaneous evaporation $\frac{\mathrm{d}m}{\mathrm{d}t}$ for a diameter D', which lies between D_0 and D_1. It was set $D' = \frac{D_0+D_1}{2}$. According to this approach, the relative error γ of D' depends on the fraction
$phi = \frac{D_0-D_1}{D_0}$, by which the initial diameter has decreased, and on the form of the wind factor f. For no wind condition ($f = 1$) and for high wind speeds ($f = k \cdot \sqrt{\mathrm{Re}}$ according to theory and, as will be shown later, also according to experiment) one obtains by integrating Equation 1.2 respectively

$$\gamma = \frac{\phi^2}{3 \cdot (2-\phi)^2} \quad \text{and} \quad \gamma = \frac{\phi^2}{8 \cdot (2-\phi)} \,.$$

For $\phi = 0.3$ the expressions become equal to 1.0 and 0.7 %. If the diameter is not reduced by more than 30 %, one can therefore take the mean value of the diameter with an error of $\leq$1 %.
When determining the mass reduction δm, it became apparent that measuring the average diameter before and after evaporation did not provide sufficiently precise values. Therefore, δm was determined by integration, which was quite time-consuming but gave very reliable results. The drop was a body of revolution whose axis passed through the center of the suspension device. The reduction in the cross-section perpendicular to the axis was measured at different heights with the comparator and δm was then found by geometric integration.
The values for the diameter before and after evaporation were determined in the following manner. According to the photographs of the drops, the lower half of the drop (counting from the largest cross section) was the most spherical in shape. Since evaporation was greatest here, the mean value of the three main axes of the lower half was used as the diameter. At no wind, this application of the mean value can easily be justified. According to Jeffrey ([21]), because of the identity of the electrostatic equations with those of diffusion for bodies of any shape, one can replace the radius r in Equation 1.1 with the capacity of the evaporating surface. If one views the drop as an elongated ellipsoid of revolution, one can show from the well-known capacity formula (e.g. according to Becker ([10])) that the capacity corresponds to the average of the three main axes up to fairly large deviations from the spherical shape. In the case of wind, where the calculation is very difficult, one can expect that the same averaging can be used for small deviations from the spherical shape. For the solid naphthalene spheres, the evaporation was measured radially for various θ (see 12) by placing a rotatable microscope stage on the comparator and attaching the plates to the stage. The evaporation at various points was indicated here by the dimensionless mass transfer number Nu′ (corresponding to the Nusselt number Nu for heat transfer). It was

$$\mathrm{Nu}' = \frac{\partial^2 m}{\partial F \, \partial t} \cdot \frac{D}{\mathscr{D} \, c_m} \,. \tag{3.2}$$

For different Re numbers, Nu′ was recorded as a function of the angle θ. The total evaporation was also calculated here by graphical integration.
So, the values $\frac{\mathrm{d}m}{\mathrm{d}t}$, D, U and the corresponding values of air pressure and temperature are measured. When testing the theory, the wind factor f should be represented as a function of Re for various σ. Re was calculated from the equation $\mathrm{Re} = \frac{\rho U D}{\eta}$ as above. The kinematic viscosity $\nu = \frac{\eta}{\rho}$ was taken from a diagram ([42]) for the air pressure and temperature values in question. According to the kinetic gas theory, $\sigma = \frac{\mathscr{D}}{\nu}$ is independent of pressure and temperature and is therefore characteristic for every substance. In the expression for $\frac{\mathrm{d}m}{\mathrm{d}t}$, according to Equation 1.2, the diameter is not only included in f. To obtain the wind factor, one must divide the measured $\frac{\mathrm{d}m}{\mathrm{d}t}$ by the value obtained for the same D when there is no wind. It was therefore advisable to introduce a different evaporation measure that gave the same function of f for all droplet sizes. This is the case with the expression $\frac{\mathrm{d}D^2}{\mathrm{d}t}$ (the reduction in diameter squared per second). It results in (ρ_1 = droplet density):

$$\frac{\mathrm{d}D^2}{\mathrm{d}t} = \frac{4}{\pi \rho_1 D} \cdot \frac{\mathrm{d}m}{\mathrm{d}t} \,. \tag{3.3}$$

According to Equation 1.2 the following holds:[1]

$$\frac{\mathrm{d}D^2}{\mathrm{d}t} = \frac{8\,\mathscr{D}\,\mathscr{M}\,p}{\rho_1\,\mathscr{R}\,T} \cdot f \tag{3.4}$$

or

$$\frac{\mathrm{d}D^2}{\mathrm{d}t} = \left(\frac{\mathrm{d}D^2}{\mathrm{d}t}\right)_0 \cdot f \,. \tag{3.5}$$

Here $\left(\frac{\mathrm{d}D^2}{\mathrm{d}t}\right)_0$ is the value obtained for no wind regardless of the droplet size. To make the values of $\frac{\mathrm{d}D^2}{\mathrm{d}t}$ comparable, they were converted to the same outside temperature (20 °C) and pressure (760 mm Hg) while keeping f constant. It is easy to see (because $\mathscr{D}$ is approximately proportional to $\frac{T^2}{B}$; B = atmospheric pressure) that one has to multiply the $\frac{\mathrm{d}D^2}{\mathrm{d}t}$ values by

$$\frac{B}{760} \cdot \frac{293 \cdot p_{20}}{T \cdot p}$$

when converting the above mentioned values. The way in which the percentage change in the temperature correction factor $\frac{293 \cdot p_{20}}{T \cdot p}$ per degree was determined for the different substances depended on which material constants were known. Since the temperature deviations from 20 °C were usually only a few tenths, the correction did not have to be known with great precision. For aniline it was calculated using Clapeyron's formula from the heat of vaporization (104.3 at

[1] Because D and m are reduced during evaporation, a minus sign should actually be included in the formulas for $\frac{\mathrm{d}D^2}{\mathrm{d}t}$ and $\frac{\mathrm{d}m}{\mathrm{d}t}$, but this is omitted for reasons of convenience.

181 °C ([1]); 133.6 at 102 °C ([3]); ∴ approximately 164 g cal g^{-1} at 20 °C) at 9 % per degree. For naphthalene it was obtained from a vapor pressure formula ([53]) $\left(\log(p_m) = -\frac{3729}{T} + 11.450\right)$ at 10 % per degree. Finally, for nitrobenzene it was calculated from the vapor pressure values ([4]) at 15, 20 and 25 °C to be approximately 6 % per degree. The systematic error that arose when reducing to the common outside temperature (20 °C) due to the dependence of the droplet cooling on wind speed etc. could be neglected for naphthalene and nitrobenzene, and was anticipated for aniline by reducing the no wind condition value by 1.5 % (cf. subsection 3.2.10). For water where p, which equals the difference between the vapor pressure at the surface (approximately saturation pressure at the droplet temperature) and that in the air (measured with the Assmann psychrometer) was known, the quantity $\frac{\mathrm{d}D^2}{\mathrm{d}t} \cdot \frac{1}{p}$ was used instead of $\frac{\mathrm{d}D^2}{\mathrm{d}t}$. A temperature correction was not necessary here because T (here the mean of droplet temperature and air temperature) was 288 °C to 290 °C in all experiments. For water, however, a correction was made due to incomplete saturation on the surface (see subsection 3.2.5 below).

3.2 Discussion of some Sources of Error

Some sources of error apart from those discussed earlier will be discussed below, the influence of which complicates the problem and possible deviations between the theory and the experiments are to be expected. If a source of error affected the evaporation rate by no more than 1 %, no correction was usually applied.

3.2.1 Deviations due to Liquid State of the Drops

It was assumed that the drops could be treated like solid spheres. Rayleigh theoretically and Ph. Lenard investigated the shape of a falling drop experimentally with good agreement ([9]). The drop carries out oscillations of different orders (n). If τ_n = oscillation time, m = droplet mass and H = surface tension, the following formula is obtained for small amplitudes:

$$\tau_n = \sqrt{\frac{3\pi}{n \cdot (n-1) \cdot (n+2)} \cdot \frac{m}{H}}\,. \tag{3.6}$$

For $n = 1$ there is no movement, the drop is spherical. For $n = 2$ one gets approximately ellipsoidal oscillations and for higher n more complicated shapes. Due to internal friction, a smaller amplitude can be expected for small drops than for large ones. If the amplitude is noticeable, but the oscillation time τ_n is greater than the time τ during which the air flows through a path equal to the diameter, the flow probably follows the oscillating motion of the surface in a quasi-stationary manner, and no great change can be expected for evaporation. For water, the

r, (cm)	velocity, ($\mathrm{cm\,s^{-1}}$)	τ_2, (sec)	τ, (sec)
0.01	69	$0.26{\cdot}10^{-3}$	$0.29{\cdot}10^{-3}$
0.03	247	$1.4{\cdot}10^{-3}$	$0.24{\cdot}10^{-3}$
0.1	676	$8.3{\cdot}10^{-3}$	$0.30{\cdot}10^{-3}$

Table 3.1: Calculated values for τ_2 and τ for water

values for τ_2 and τ are obtained as shown in Table 3.1.

To calculate τ, speed values were taken from a table in an earlier paper of mine about the falling speed of the sphere ([16]).

For radii over 0.03 cm, the oscillations become so slow that they have no effect even at noticeable amplitudes (but not too large ones), and for smaller drops the amplitudes probably become small. For radii >0.1 cm one can possibly expect such large amplitudes that significant deviations occur. It was assumed here that the ellipsoidal oscillations predominate, which is motivated by the fact that the higher oscillations are damped more strongly due to the higher frequency. Thus, for falling drops of the same size as those discussed in this paper, one can expect the same evaporation as for solid spheres.

The transport to the surface layer is low because the ratio between the viscosity of the liquid and that of the air is high. For water it is about 50, for nitrobenzene it is ∼100 and for aniline it is ∼250.

If the drop is suspended on a glass thread or a thermocouple, as in these experiments, the deviations from the conditions for the solid sphere are not the same as those for the falling motion, but they are of the same order of magnitude. The above-mentioned reasons why the evaporation in the latter case is about the same as for a solid sphere are not strict, but as the same laws are obtained in the experiments for the liquid drops as for the naphthalene spheres, there is strong confirmation in this. In my previously mentioned paper ([16]) I showed that water drops with radii <0.75 mm obey approximately the same law of falling bodies as solid spheres.

3.2.2 The Effect of Turbulence

Previously it was mentioned that based on smoke tests the wind tunnel provided a quiescent stream. An investigation into the influence of remaining turbulence on total evaporation was carried out by measuring $\frac{\mathrm{d}D^2}{\mathrm{d}t}$ for approximately the same drop diameter (0.6 mm) and the same wind speed ($1\,\mathrm{m\,s^{-1}}$) using three nozzles. With this three nozzles the degree of turbulence was different. It turned out that for nitrobenzene the deviations from the empirical law mentioned later for the

nozzle diameters 20, 16 and 10 cm were +2.1 %, +1.6 % and +0.1 %, respectively. Since, as mentioned later, the average deviation in the nitrobenzene tests was 1.6 %, these differences are within experimental error. In this case, turbulence can therefore be neglected.

3.2.3 The Compressibility of Air

When drawing up the equations for the flow, it was assumed that the air was incompressible. The relative variations in air density as a result of the pressure distribution could be neglected because the dynamic pressure at the highest speeds ($<12\,\mathrm{m\,s^{-1}}$) was less than 0.7 mm Hg and the pressure variations, for example according to Krell ([22]), are of the order of magnitude of the dynamic pressure. The air could therefore be considered incompressible when calculating the velocity field. The pressure-dependent material constants (e.g. $\mathscr{D}$) were the same everywhere.

3.2.4 The Non-Stationary State

It was assumed that evaporation was stationary. The flow became stationary very quickly because the flow traveled a distance every second that was very large in relation to the diameter (e.g. Boltze ([11])). The non-stationary problem has been treated for quiescent wind by Fuchs ([17]). He gives the following formula (changed according to my terms):

$$\frac{\mathrm{d}m}{\mathrm{d}t} = \left(\frac{\mathrm{d}m}{\mathrm{d}t}\right)_S \cdot \left(1 + \frac{r}{\sqrt{\pi t\,\mathscr{D}}}\right) . \tag{3.7}$$

Here $\left(\frac{\mathrm{d}m}{\mathrm{d}t}\right)_S$ is the evaporation at a stationary state; at $t = 0$ the vapor concentration is zero everywhere. By integrating Equation 3.7 one obtains (assuming r to be constant):

$$\delta m = (\delta m)_S \cdot \left(1 + \frac{2r}{\sqrt{\pi t\,\mathscr{D}}}\right) .$$

The term $\frac{2r}{\sqrt{\pi t\,\mathscr{D}}}$ gives the error that is obtained if one treats the measured evaporation $\frac{\mathrm{d}m}{\mathrm{d}t}$ as stationary. One can easily calculate the smallest fraction of the drop that must evaporate in order for this error (ε) to be less than 1 %. So we have:

$$t = \frac{4r^2}{\varepsilon^2 \pi\,\mathscr{D}} = \frac{\rho_1\,\mathscr{R}\,T}{\mathscr{D}\,\mathscr{M}\,p} \cdot r\delta r$$
$$\therefore \frac{\delta r}{r} = \frac{4\,\mathscr{M}\,p}{\varepsilon^2 \pi\,\mathscr{R}\,T\rho_1} .$$

In the experiments one gets for $\frac{\delta r}{r}$ the following values for water 6.5 %, aniline = 2.7 %, nitrobenzene = 1.8 % and naphthalene = 0.4 %. In fact, the deviations from the stationary state are smaller because a certain vapor envelope is always carried

along with the drop. When measuring evaporation in moving air, the deviations are likely to be even smaller because the concentration gradient is smaller and therefore not as much needs to evaporate in order to provide the necessary concentration field. Although some of the vapor is partly carried away, the magnitude is unlikely to change. So far, the non-stationary state, which lies in the decreasing of the droplet, has not been taken into account. Fuchs ([17]) treated this factor for quiescent wind and, according to his calculations, this did not change the magnitude of the deviations.
The process could therefore be viewed as stationary in the experiments, which incidentally also emerged from the fact that $\frac{\mathrm{d}D^2}{\mathrm{d}t}$ proved to be constant as evaporation continued.

3.2.5 The Vapor Pressure at the Surface

The existence of saturation pressure on the surface was assumed as a boundary condition for the evaporation experiments. The correctness of this assumption is examined below. This partly follows a line of thought developed by Müller-Pouillets ([31]) for evaporation in a vacuum. If the number of vapor molecules present close to the surface in one cubic centimeter is set equal to N, their average speed is $\overline{U}$ and their average path length is l_1, then according to Jäger ([20]) the number of vapor molecules hitting the surface per second and square centimeter is equal to

$$\frac{N\overline{U}}{4} + \frac{\overline{U}l_1}{6} \cdot \frac{\partial N}{\partial n} .$$

For the mass $\left(\frac{\partial^2 m}{\partial F\,\partial t}\right)_1$ hitting every square centimeter every second, one easily obtains at small vapor pressure values using the well-known formula for $\overline{U}$, because $\mathscr{D} = \frac{l_1\overline{U}}{3}$

$$\left(\frac{\partial^2 m}{\partial F\,\partial t}\right)_1 = \sqrt{\frac{\mathscr{M}}{2\pi\,\mathscr{R}\,T}} \cdot p_0 - \frac{1}{2}\,\mathscr{D} \cdot \frac{\partial c}{\partial n} .$$

Here p_0 is the vapor pressure in the layer close to the surface. If the fraction α of the molecules is absorbed by the surface (α = "evaporation coefficient"), the condensation becomes equal to

$$\alpha \cdot \left(\sqrt{\frac{\mathscr{M}}{2\pi\,\mathscr{R}\,T}} \cdot p_0 - \frac{1}{2}\,\mathscr{D} \cdot \frac{\partial c}{\partial n}\right) .$$

So for saturated vapor, if the evaporation is equal to the condensation and $\frac{\partial c}{\partial n} = 0$, the evaporation will be equal to

$$\alpha \cdot \sqrt{\frac{\mathscr{M}}{2\pi\,\mathscr{R}\,T}} \cdot p_m \,, \tag{3.8}$$

p_m being the saturation pressure. Since this evaporation does not depend on the partial pressure p_0 of the vapor, the evaporation (the part that is carried away from the surface) becomes

$$\left(\frac{\partial^2 m}{\partial F\,\partial t}\right) = \alpha \cdot \sqrt{\frac{\mathscr{M}}{2\pi\,\mathscr{R}\,T}} \cdot (p_m - p_0) - \frac{\alpha}{2}\,\mathscr{D} \cdot \frac{\partial c}{\partial n}\,.$$

Because

$$\left(-\,\mathscr{D} \cdot \frac{\partial c}{\partial n}\right) = \left(\frac{\partial^2 m}{\partial F\,\partial t}\right)\,,$$

there results

$$\left(\frac{\partial^2 m}{\partial F\,\partial t}\right) = \frac{\alpha}{1 - \frac{\alpha}{2}} \cdot \sqrt{\frac{\mathscr{M}}{2\pi\,\mathscr{R}\,T}} \cdot (p_m - p_0)\,. \tag{3.9}$$

The equation differs from the one that applies at very low pressure in the denominator $\left(1 - \frac{\alpha}{2}\right)$. The question of whether α has changed due to the presence of air is difficult to answer. Air molecules may adsorb to the surface, making it more difficult for the molecules to pass through and α decreases. For reasons that will be mentioned later, the same α is used as for vacuum. At steady state, if one takes Nu' from the defining Equation 3.2, there results (c_m ist replaced by $c_0 - c'$):[2]

$$\begin{aligned}
&\frac{\alpha}{\left(1 - \frac{\alpha}{2}\right)} \cdot \sqrt{\frac{\mathscr{M}}{2\pi\,\mathscr{R}\,T}} \cdot (p_m - p_0) = \frac{\mathscr{D} \cdot (c_0 - c') \cdot \mathrm{Nu}'}{D} \\
&\because \frac{(p_m - p_0)}{(p_0 - p')} = \frac{2 - \alpha}{2\alpha} \cdot \frac{\sqrt{2\pi\,\mathscr{M}} \cdot \mathscr{D} \cdot \mathrm{Nu}'}{D \cdot \sqrt{\mathscr{R}\,T}} = K \cdot \mathrm{Nu}'\,.
\end{aligned} \tag{3.10}$$

Here $\frac{(p_m - p_0)}{(p_0 - p')}$ at small $(p_m - p_0)$ is the relative correction due to incomplete saturation on the surface. Because Nu' varies over the surface, one must use the mean value $\overline{\mathrm{Nu}}'$ for this quantity in Equation 3.10. It is obtained from the following equation:

$$\overline{\mathrm{Nu}}' = \frac{1}{F} \cdot \int \mathrm{Nu}' \cdot (1 - K \cdot \mathrm{Nu}')\,\mathrm{d}F = \frac{1}{F} \cdot \left[\int \mathrm{Nu}'\,\mathrm{d}F - K \cdot \int \mathrm{Nu}'^2\,\mathrm{d}F\right]\,.$$

So the relative correction (ω) for the mean Nu' and so for $\frac{\mathrm{d}D^2}{\mathrm{d}t}$ becomes

$$\omega = K \cdot \frac{\int \mathrm{Nu}'^2\,\mathrm{d}F}{\int \mathrm{Nu}'\,\mathrm{d}F}\,. \tag{3.11}$$

The correction ω depends on the distribution of Nu' over the surface. We deal with two simple cases here:

[2] As on page 10, footnote, c' and p' are the concentration and pressure in undisturbed air.

1. The distribution over the surface is constant (as with no wind):

$$\omega = K \cdot \overline{\mathrm{Nu}}' .$$

Because $\overline{\mathrm{Nu}}'$ is equal to $2 \cdot f$ according to Equation 3.2, one gets in this case

$$\omega = 2 \cdot K \cdot f . \tag{3.12}$$

2. In the Nu'-$\cos(\theta)$ diagram (used in calculating total evaporation for naphthalene), Nu' falls linearly from a maximum value ($2 \cdot \mathrm{Nu}'$) at the forward stagnation point to zero at the rear. This should correspond to the distribution in strong winds. Although (as will be discussed later) Nu' falls to a minimum value below the equator and then rises; but the integrals appearing in Equation 3.11 retain approximately the same values due to this simple assumption. In this case one gets

$$\omega = \frac{4}{3} \cdot K \cdot \overline{\mathrm{Nu}}' = \frac{8}{3} \cdot K \cdot f . \tag{3.13}$$

Equation 3.12 and Equation 3.13 are almost the same. The variations that occur in the Nu' distribution are therefore irrelevant for calculating the correction. When there is no wind one can use Equation 3.12 (which gives $\omega = 2 \cdot K$) and when there is wind one can use Equation 3.13.
Unfortunately, the evaporation coefficient α is only known for a few substances. For water, Alty and MacKay ([7]) obtained $\alpha = 0.036$ for small pressure values. For several metals α is very close to 1 and for benzophenone $0.2 - 0.5$ (Intern. Crit. Tab.). For carbon tetrachloride, $\alpha = 1$ (Alty ([8])).
For the water tests, the correction for $\alpha = 0.036$ is a maximum of 6 %. The values were converted taking this correction into account. No corrections were made for naphthalene, nitrobenzene, and aniline because α is unknown and (since these substances are more closely related to carbon tetrachloride and benzophenone) probably much larger than for water. By the way, a large correction would destroy the accuracy with which the similarity laws apply according to the experiments (see below), which supports the correctness of this assumption of a small correction.
Mache ([28]) found a difference between the saturation pressure and the generating pressure at the surface when measuring diffusion constants using Winkelmann's method. According to my Equation 3.9, he assumed a proportionality between $\frac{\partial^2 m}{\partial F \, \partial t}$ and $(p_m - p_0)$. However, according to his experiments at 27 °C, a proportionality factor was obtained for water that is approximately 16 times smaller than that calculated from my formula. This would make the correction 16 times greater than that obtained here. The following facts can be cited to decide this question:

1. In the Mache experiments, the evaporation of water in a cylindrical tube was determined as a function of the distance (h) of the surface from the

free end of the tube, where the vapor concentration was set to zero. The following relationship was obtained between the evaporation time τ (the time for evaporation of 1 mm of water) and the height h: $\tau = A + B \cdot h$.
Here A and B are constants, at least B of which depends on the temperature. The large vapor pressure difference at the surface was noted because of the appearance of the number A. However, the effect is greatly reduced if one assumes that the real value of h is slightly larger than the pipe length, which could depend on the fact that there is no complete compensation at the mouth. When water evaporated into air, A/B became equal to 4 mm at 92.4 °C, 2.8 mm at 87.8 °C and 0.08 mm at 27.5 °C. The value of h only needed to be increased by these lengths, which seems plausible since the inner tube diameter was 2.7 mm. An incomplete temperature equilibration on the water surface also gives rise to an apparent difference. MACHE's experiments therefore cannot draw any precise conclusions about the actual vapor pressure difference.

2. One might expect that by measuring the moisture boundary layer one could find the vapor pressure difference at the surface with sufficient accuracy. BÜTTNER ([12]) has published some such measurements, but the boundary layer thickness was so great that the pressure difference $(p_m - p_0)$ according to MACHE was only 1 % of the vapor pressure difference $(p_0 - p')$ and therefore could not be reliably verified. To obtain larger differences, one would have to use boundary layers so thin that the hygrometer would produce large deviations.

3. In my experiments, good agreement with the similarity theory was obtained. If the correction had to be applied according to MACHE, values would be obtained for the largest drops ($D = 1.8$ mm) that would be ∼25 % more than those for the smallest ($D = 1.0$ mm). This therefore suggests that the correction with the value $\alpha = 0.036$ is of the correct order of magnitude.

4. The temperatures of the water drops, measured with a thermocouple, were only a few tenths of a degree higher than those of the moisty psychrometer thermometer, although the temperature difference was approximately 7 °C to 10 °C. Since the cylindrical mercury container of the psychrometer had a length of 15 mm and a diameter of 4 mm, a much smaller vapor pressure difference $(p_m - p_0)$ would have been expected for the psychrometer than for drops. According to MACHE's results, an apparent psychrometer constant would be expected for the drops that would have to be approximately twice as large as the usual one, which would correspond to a temperature difference of several degrees compared to the moisty psychrometer thermometer. By the way, if the larger correction were used, an increase in the droplet temperature would be expected with increased wind speed. In fact, the opposite (as with the psychrometer) has been observed. Because of the above-mentioned facts,

the appropriate correction (with $\alpha = 0.036$) was assumed to be at least approximately correct.

3.2.6 The Purity and Stability of the Substances

The purest KAHLBAUM's preparations were used in the experiments without any further purification procedures. One might expect that if the substances were not completely pure, large errors would occur when determining evaporation. But even if the vapor pressure were reduced by 10 % due to impurities, the vapor pressure would only change by about 3 % during the experiment because the drop radius was usually reduced by about 10 %, i.e. the volume was reduced by about 1/4. With this large impurity, the average vapor pressure would only change by 1.5 %, and the same vapor pressure would be present in all experiments (decreased by around 11 % everywhere), which is why there can be no effect on the derived laws. Even if the material were not completely stable, a reduction in vapor pressure could occur, but this is difficult to predict. The fact that there were no deviations in the experiments due to a lack of purity or stability can be seen from the fact that no deviations occurred when the same drop was repeatedly evaporated and that the values at the end of the series of tests agreed well with those obtained first.

3.2.7 The Effect of Surface Curvature on the Vapor Pressure

Because of the curvature, the vapor pressure and therefore the rate of evaporation are increased for very small drops. However, using the well-known THOMSON's law, one can easily show that this change has no effect whatsoever on the drop sizes used in these experiments. Although THOMSON's law was criticized by SCHREBER ([43]) (e.g. it should lead to a perpetual motion machine) and replaced by a slightly modified one, but this did not change the magnitude of the increase in vapor pressure.

3.2.8 The Validity of the Laws of an Ideal Gas

In the previous calculations, the equation $c_m = \frac{\mathscr{M} p}{\mathscr{R} T}$ was used for vapor even though it was fully or nearly saturated. The fact that the error is at most 0.5 % for temperatures below 40 °C was shown for water by comparing the calculated values with experimental ones ([5]). For the other substances used, the deviations must be even smaller because they have much higher boiling points.

3.2.9 Is the Vapor Pressure Negligible Compared to the Air Pressure?

It was previously assumed that evaporation was proportional to the vapor pressure difference. However, this only applies to low vapor pressure values. For larger ones

it becomes proportional to the expression $B \cdot \log \left[\frac{(B-p')}{(B-p_0)} / \right]$ (STEFAN).[3] Developed in a TAYLOR series, one gets:

$$(p_0 - p') + \frac{p_0^2 - p'^2}{2B} + \cdots$$

At small vapor pressure the expression is $(p_0 - p') = p$. The percentage deviation from this is, to a first approximation, $\frac{p_0 - p'}{2B}$. Since the average value $\frac{p_0 + p'}{2}$ in the water tests was <9.5 mm Hg, this deviation amounts to a maximum of 1.3 % and was therefore not taken into account.

3.2.10 The Reduction in Temperature of the Drops

In the experiments with nitrobenzene, aniline and naphthalene, the evaporation values were converted to a common air temperature. The error that occurred is calculated below. A temperature equilibrium is achieved when the amount of heat removed from the drop per second is equal to that supplied during the same time. The first quantity mentioned is

$$= l \cdot \frac{\mathrm{d}m}{\mathrm{d}t} = 4\pi \cdot \mathscr{D} \cdot \frac{\mathscr{M}\, p}{\mathscr{R}\, T} \cdot rlf$$
$$l = \text{ specific heat of vaporization,}$$

bound during evaporation. The latter part is composed of four parts:

1. The heat supplied by conduction and convection, which is equal to $4\pi \cdot \lambda \cdot r \cdot \theta \cdot f_1$ due to the analogy of heat and mass transfer. Here λ is the thermal conductivity; θ the temperature reduction; f_1 is the wind factor for the case that $\sigma_1 = \frac{\lambda}{\nu c_p \rho}$ (see chapter 2).

2. The heat supplied by radiation. Since the dependence of the drop's absorption coefficient on wavelength and temperature is unknown, this heat cannot be calculated precisely, but an upper limit can be obtained by considering the drop as a black body. If the STEFAN-BOLTZMANN constant($1.374 \times 10^{-12}\,\mathrm{g\,cal\,cm^{-2}\,s^{-1}\,grad^{-1}}$ ([21])) is denoted by $\overline{\sigma}$, the heat supplied per side by radiation is equal to
$$4\pi r^2 \cdot 4T^3 \cdot \overline{\sigma} \cdot \theta \cdot a\,,$$
where a is a number < 1.

3. The heat supplied by the glass thread. It is,
$$\pi r_1^2 \cdot \frac{\theta}{a_2 \cdot r} \cdot \lambda_1\,,$$

[3] The definition of p_0 and p' follows from subsection 3.2.5

where r_1 is the radius of the glass thread, λ_1 is the thermal conductivity of the glass and a_2 is the difficult-to-determine fraction of the radius at which the temperature drop θ occurs (estimated at $\sim$1).

4. The heat developed by the friction of air. Only a very small part of it reaches the drop. The residue is carried away by the air. To get an upper limit, one calculates the total heat developed. If the drag number is c, the resistance becomes $\frac{1}{2} \cdot c\pi r^2 \cdot \rho U^2$, and the heat removed per second from the flow energy becomes

$$\frac{c\pi r^2 \cdot \rho U^3}{2J},$$

(J = mechanical heat equivalent). The heat transferred to the drop is

$$\frac{a_1 \cdot c\pi r^2 \cdot \rho U^3}{2J},$$

where a_1 is a number much smaller than 1. At large Re numbers, a large part of the energy is used in the vortex movement, which is only dampened far away from the drop.

By equating the heat supplied with the heat removed, an equation is obtained from which the temperature reduction θ can be calculated. It becomes when

$$\frac{8\,\mathscr{D}\,\mathscr{M}\,p}{\rho_1\,\mathscr{R}\,T} = \left(\frac{\mathrm{d}D^2}{\mathrm{d}t}\right)_0 \tag{3.14}$$

is set:

$$\theta = \frac{\rho_1 l}{8\lambda} \cdot \frac{f}{f_1} \cdot \frac{\left(\frac{\mathrm{d}D^2}{\mathrm{d}t}\right)_0 - \frac{a_1 \cdot cr \cdot \rho U^3}{J\rho_1 l f}}{1 + \frac{4T^3 \cdot \overline{\sigma} a}{\lambda} \cdot \frac{r}{f_1} + \frac{r_1^2 \lambda_1}{4r^2 \lambda a_2 f_1}}. \tag{3.15}$$

For $\lambda = 0.000\,060\,\mathrm{g\,cal\,cm^{-1}\,s^{-1}\,grad^{-1}}$, ([2]), the second term of the denominator for the largest r (0.9 mm) is equal to $0.21 \cdot \frac{a}{f_1}$, i.e. always ≤ 0.2. The third term of the denominator is smaller than $0.09 \cdot \frac{1}{a_2 f_1}$ for the values for $\frac{r_1}{r}\left(< \frac{1}{10}\right)$ and $\lambda_1 = 0.0022$ used in the aniline experiments (in which the cooling is greatest and therefore the magnitude of the various terms is most important). The ratio between the second and first terms of the numerator is $0.09 \cdot a_1$ for aniline for the largest Re numbers (with the second term being the largest). Because of the smallness of the number a_1, the second term of the numerator can always be neglected. For the upper limit of θ the formula

$$\theta_{\text{max.}} = \frac{\rho_1 l}{8\lambda} \cdot \left(\frac{\mathrm{d}D^2}{\mathrm{d}t}\right)_0 \cdot \frac{f}{f_1} \tag{3.16}$$

results. For large Re numbers, this formula applies very precisely because f and f_1 appear in the denominators of the neglected fractions, $\frac{f}{f_1}$ is here (according to the

	at no wind		at large Re numbers	
material	$\theta_{\text{max.}}$	θ, measured	$\theta_{\text{max.}}$	θ, measured
aniline	0.42 °C	0.32 °C	0.61 °C	0.49 °C
nitrobenzene	0.12 °C	0.12 °C	0.19 °C	0.21 °C
naphthalene	0.048 °C	–	0.074 °C	–

Table 3.2: Measured and calculated values of θ for the materials used

experiment) equal to

$$\frac{k \cdot \sqrt{\text{Re}}}{k_1 \cdot \sqrt{\text{Re}}} = \sqrt[3]{\frac{\sigma_1}{\sigma}}\,;(\sigma_1 = 1.4)\,.$$

When there is no wind ($f = f_1 = 1$), the results from Equation 3.16 are less than $^1/_5$ too large because of the second term in the denominator. It is noteworthy that Equation 3.16 gives the same cooling rate for all droplet sizes for given Re numbers. For the different materials, the $\theta_{\text{max.}}$ values for no wind and for large Re numbers were calculated according to Equation 3.16. $\left(\frac{\mathrm{d}D^2}{\mathrm{d}t}\right)_0$ was obtained from the measurements at no wind. The heat of vaporization used for aniline was $164\,\mathrm{g\,cal\,g^{-1}}$ (from subsection 3.1.8) and for nitrobenzene and naphthalene the values used were 77 and 133 (according to the vapor pressure values already cited). The values listed later (Table 4.2) were used for σ. As a control, θ was determined for aniline and nitrobenzene by placing a drop of these substances on one soldering point of the thermocouple and a drop of paraffin oil on the other. The inertia of the temperature fluctuations was obtained with the paraffin oil drops, which could not have a noticeable cooling rate. Although the data had to result in values that were somewhat too small (due to the greater thermal conductivity of constantan and manganine) and the possible errors in the data had to be somewhat larger than 0.05 °C, the magnitude could still be checked. Table 3.2 gives a comparison of the calculated and measured values. The calculated and measured values agree well.

As mentioned above (subsection 3.1.8), when converting to 20 °C outside temperature for aniline, nitrobenzene and naphthalene, the corrections 9, 6 and 10 % per degree were used. Table 3.2 shows that cooling the drops of aniline caused changes of several percent in the evaporation $\frac{\mathrm{d}D^2}{\mathrm{d}t}$. Since only the differences in the θ values are important when determining f, the $\frac{\mathrm{d}D^2}{\mathrm{d}t}$ values for aniline were reduced by 1.5 % for no wind conditions (actually 0.18×9) and thus all drops were reduced to a drop temperature of approximately 19.5 °C. Although the θ values for the smallest Re numbers lie between those given in Table 3.2, the deviation is insignificant because an error in θ of 0.11 °C only accounts for 1 %. The corresponding

correction was not applied to nitrobenzene because it is only $0.07 \times 6 = 0.4\,\%$. So the average temperature of the nitrobenzene drops was 19.84 °C. Also no correction was necessary for naphthalene; the average temperature was 19.94 °C.

3.2.11 The Effect of the Suspension Device

Due to the wetting of the glass thread or metal wire, the spherical shape of the drops was slightly disturbed (Figure 3.2, 4 to 11). This disturbance was greatest on the upper side (i.e. on the leeward side) due to gravity. Because the evaporation here was relatively small, only a very small effect of the disturbance on the results was expected. On the other hand, a small peak (due to the protrusion of the suspension device) was often created, which was subtracted when measuring the D. The fact that this peak was without influence is evident from the fact that the same $\left(\frac{\mathrm{d}D^2}{\mathrm{d}t}\right)$ was measured for drops without peaks. However, if the drop had decreased in size so much that the deviation from the spherical shape was too great (Figure 3.2, 8), it was no longer measured. The fact that no significant disturbance occurred in the dimensions of the suspension device used (as expected) is evident from the fact that with variations of the glass thread diameter and a constant drop size, there was no change in $\left(\frac{\mathrm{d}D^2}{\mathrm{d}t}\right)$. From the facts stated above it is clear that, despite the number of complicating factors, one can expect good agreement with the results obtained in the theoretical part. The calculations in subsection 3.2.5 was partly based on the assumption that the similarity conditions would be confirmed in the experiments, but because this was in fact the case (see below), one could also expect agreement for the remaining theoretical results.

4 Experimental Results

4.1 Measurement of the Total Evaporation

4.1.1 At No Wind

The following $\left(\frac{\mathrm{d}D^2}{\mathrm{d}t}\right)$ values (reduced to 760 mm Hg air pressure and 20 °C outside temperature) were obtained for nitrobenzene in calm wind conditions. As stated above (subsection 3.1.7) among the reasons for permissible neglect of the influence of convection, the measured $\left(\frac{\mathrm{d}D^2}{\mathrm{d}t}\right)$ values are independent of r, although r was varied more than in the ratio 1 : 2, see Table 4.1. The following mean value (with the average error indicated) was obtained

$$\left(\frac{\mathrm{d}D^2}{\mathrm{d}t}\right)_0 = (0.651 \pm 0.004) \cdot 1 \times 10^{-6}\,\mathrm{cm^2\,s^{-1}}\,.$$

According to the formula

$$\left(\frac{\mathrm{d}D^2}{\mathrm{d}t}\right)_0 = \frac{8\,\mathscr{D}\,\mathscr{M}\,p}{\rho_1\,\mathscr{R}\,T}$$

$\mathscr{D}$ was calculated using the value of the vapor pressure given in subsection 3.1.8. Since the droplet temperature was 19.84 °C (according to subsection 3.2.10), the vapor pressure was $0.262 \cdot (1 - 0.06 \cdot 0.16) = 0.259$ mm Hg. The value $\mathscr{D} = 0.0560$ was obtained. For aniline the result was

$$\left(\frac{\mathrm{d}D^2}{\mathrm{d}t}\right)_0 = (1.210 \pm 0.022) \cdot 1 \times 10^{-6}\,\mathrm{cm^2\,s^{-1}}\,.$$

The droplet temperature was 19.5 °C (according to subsection 3.2.10). When measuring the diffusion constants of various substances, Mack ([29]) found values

r, (µm)	172	175	233	295	301	361
$\left(\frac{\mathrm{d}D^2}{\mathrm{d}t}\right)_0 \cdot 10^9$, (CGS.)	652	654	639	650	658	652

Table 4.1: Variation of r and corresponding $\left(\frac{\mathrm{d}D^2}{\mathrm{d}t}\right)$

for evaporation from a flat surface through a pipe at 25 °C, which can be used to calculate the $\left(\frac{\mathrm{d}D^2}{\mathrm{d}t}\right)_0$. One gets $2.02 \times 10^{-6}\,\mathrm{cm^2\,s^{-1}}$. With the correction of 9 % per degree one gets with a drop temperature of 19.5 °C

$$2.02 \cdot e^{-0.09 \cdot 5.5} \cdot 10^{-6} = 1.23 \times 10^{-6}$$

The agreement is good. This was mentioned above (subsection 3.2.6) among the reasons for neglecting the influence of convection. The diffusion constant $\mathscr{D} = 0.0702$ (converted to 20 °C) calculated by Mack using a vapor pressure value determined by him is used below.
For naphtalene

$$\left(\frac{\mathrm{d}D^2}{\mathrm{d}t}\right)_0 = (0.1534 \pm 0.007) \cdot 1 \times 10^{-6}\,\mathrm{cm^2\,s^{-1}}$$

was obtained. The drop temperature was 19.94 °C (according to subsection 3.2.10). From Mack's measurements above, $\left(\frac{\mathrm{d}D^2}{\mathrm{d}t}\right)_0 = 0.308 \cdot 10^{-6}$ is obtained at 25 °C, which gives $0.186 \cdot 10^{-6}$ for 19.94 °C with a temperature correction of 10 % per degree (subsection 3.1.8). The large deviation between my value and Mack's value can be explained by the fact that his method for the examination of solid substances probably gives values that are too large due to leakage of the instrument, which Topley and Whytlaw-Gray ([52]) have shown for iodine. When studying liquids, Mack used a method in which the leakage occurred in the absorbent material and was therefore of no significance. That is why the Mack values for liquids were reliable and the above comparison for aniline is tenable. The agreement cited there as proof of the permissible neglect of convection is also valid, since such convection would give higher values for my experiments. For naphthalene, my value is used below and with the vapor pressure given in subsection 3.1.8 one obtains $\mathscr{D} = 0.0593$. Although Mack found almost the same value for 20 °C (0.0591), the agreement comes from the fact that he used a different value (from Barker) for the vapor pressure, which is probably less reliable ([53]).
No investigation was carried out for water when there was no wind, because such a precise investigation is quite difficult to carry out with my method, since due to the humidity the glass cylinder would have to be attached to the camera and the suspending device in an airtight manner and the connection with the surrounding air would have to take place through an absorption vessel. However, reliable values of the vapor pressure and the diffusion constant ([54]) for water are known enough to be able to calculate the evaporation measure $\frac{\mathrm{d}D^2}{\mathrm{d}t} \cdot \frac{1}{p}$ to be used here according to subsection 3.1.8. Because the mean of air and surface temperature (subsection 3.1.8) was 288 ° K to 290 ° K, one can use the material constants for 16 °C. With $\mathscr{D} = 0.246$ one gets $\frac{\mathrm{d}D^2}{\mathrm{d}t} \cdot \frac{1}{p} = 0.197 \times 10^{-5}\,\mathrm{cm^2\,s^{-1}\,mm\,Hg}$ for this temperature. In order to have an approximate control, $\frac{\mathrm{d}D^2}{\mathrm{d}t} \cdot \frac{1}{p}$ was determined

with the glass cylinder used for the other substances without absorbent material, with the average vapor pressure in the cylinder being calculated from the amount evaporated. The case was also examined in which a large cardboard cylinder of around $0.4\,\mathrm{m}^3$ was placed over the entire arrangement, whereby the change in humidity due to evaporation could be neglected, but the air disturbance could counteract it. The influence of free convection was not taken into account here. For example, 0.193×10^{-5} and 0.208×10^{-5} were obtained, which supports the above value. This value will also be used below.

4.1.2 In Wind

The measured evaporation $\frac{\mathrm{d}D^2}{\mathrm{d}t}$ or $\frac{\mathrm{d}D^2}{\mathrm{d}t} \cdot \frac{1}{p}$ for nitrobenzene, aniline, water and naphthalene is shown in Figure 4.1 to Figure 4.5 as a function of $\sqrt{\mathrm{Re}}$. The measurement results have also been cited above. The different drop sizes are characterized by different symbols (definition in Figure 4.1). For nitrobenzene, $\frac{\mathrm{d}D^2}{\mathrm{d}t}$ is also shown as a function of Re. From the diagrams it can be seen that the same curve was obtained for all drop sizes, and from Equation 3.5 it follows that f for a given substance only depends on the Re number. The laws of similarity are therefore precisely confirmed. The diagrams also show that the f-$\sqrt{\mathrm{Re}}$ curve is a straight line that passes through the wind rest value. So one gets:

$$f = 1 + k \cdot \sqrt{\mathrm{Re}}\,. \tag{4.1}$$

empirically. The drawn straight lines are selected appropriately based on visual judgement. The average deviation of the evaporation found from that calculated from Equation 4.1 is 1.6 % for nitrobenzene, 2.0 % for aniline, 2.4 % for water and 4.2 % for naphthalene. A larger scatter is to be expected for water than for nitrobenzene and aniline because the necessary measurement of air humidity leads to more uncertainty. With naphthalene, a fairly large scattering was also expected due to the unevenness of the surface. The investigated ranges of Reynolds numbers and drop sizes are shown in the figures. With water and naphthalene it was not possible to examine drops as small as with aniline and nitrobenzene because the suspension devices had to be quite crude. The smallest Re number was 2.27 (for nitrobenzene) and the largest was 1283 (for naphthalene). Equation 4.1 may not apply exactly due to the complicated nature of the problem, but only gives a good approximation that holds within the experimental errors.
For large Re numbers, f changes to $k \cdot \sqrt{\mathrm{Re}}$, which was to be expected from theory. For small Re numbers, f changes to 1. However, Fuchs' theory (see above) requires that $\frac{\mathrm{d}f}{\mathrm{d(Re)}} = 0$ at $\mathrm{Re} = 0$, which does not agree with Equation 4.1. But this is not a contradiction because my semi-empirical Equation 4.1 is only derived up to $\mathrm{Re} = 2$. For very small Re numbers (for which Fuchs' calculation is carried out) $\frac{\mathrm{d}f}{\mathrm{d(Re)}}$ can go towards 0 without my curve for $\mathrm{Re} > 2$ having to be changed. The investigation is therefore not considered as a test of Fuchs' theory.

substance	k	$\mathscr{D}$	$\sigma = \frac{\mathscr{D}}{\nu}$	$\log(k)$	$\log(\sigma)$	$k \cdot \sqrt[3]{\sigma}$	$k \cdot \sqrt{\sigma}$
nitrobenzene	0.378	0.0560	0.373	0.578−1	0.572−1	0.272	0.231
naphthalene	0.387	0.0593	0.395	0.588−1	0.597−1	0.284	0.243
aniline	0.358	0.0702	0.468	0.554−1	0.670−1	0.278	0.245
water	0.229	0.253	1.687	0.360−1	0.227	0.273	0.297
					mean value:	0.276	

Table 4.2: Values for k obtained from the diagrams

The various values for k in Equation 4.1 obtained from the diagrams are compiled in Table 4.2, including the σ values. The number σ, which is independent of temperature and pressure as mentioned in subsection 3.1.8, was calculated in such a way that $\mathscr{D}$ for 20 °C and 760 mm Hg (in the third column) was divided through the ν value for air at the same condition ([42]) ($0.150\,\mathrm{cm^2\,s^{-1}}$) . As can be seen from the second and fourth columns, k generally falls as σ increases, as expected from theory. Although k is a little higher for naphthalene than for nitrobenzene, the $\mathscr{D}$ are so little different that this can be explained by experimental errors.

In order to get a precise picture of the course of the $k(\sigma)$ function, one would actually have to examine some substances with $\mathscr{D}$ values that lie between those of aniline and water, but it turned out that there is none suitable material for experiments in this range. As was mentioned in the theoretical part, one can try with the function $k = \frac{\text{const.}}{\sigma^n}$. Therefore $\log(k)$ is shown as a function of $\log(\sigma)$ in Figure 4.7. From the diagram, it does not seem impossible that k can have the proposed form. The straight line drawn results in $n = 0.348$, i.e. close to $\frac{1}{3}$. The penultimate column shows that $k \cdot \sqrt[3]{\sigma}$ is well constant, while the last shows that, for example, $k \cdot \sqrt{\sigma}$ is not constant. So one gets

$$k = \frac{0.276}{\sqrt[3]{\sigma}} \tag{4.2}$$

with good agreement for the substances examined. However, the formula can also be used at least approximately for other substances, at least in the intermediate range, because k decreases with increasing σ. So one gets the final formulas (according to Equation 3.4 and according to Equation 1.2):

$$\left(\frac{\mathrm{d}D^2}{\mathrm{d}t}\right) = \frac{8\,\mathscr{D}\,\mathscr{M}\,p}{\rho_1\,\mathscr{R}\,T} \cdot \left(1 + \frac{0.276}{\sqrt[3]{\sigma}} \cdot \sqrt{\mathrm{Re}}\right) \tag{4.3}$$

or

$$\boxed{\left(\frac{\mathrm{d}D^2}{\mathrm{d}t}\right) = 4\pi \cdot \mathscr{D} \cdot \frac{\mathscr{M}\,p}{\mathscr{R}\,T} \cdot r \cdot \left(1 + \frac{0.276}{\sqrt[3]{\sigma}} \cdot \sqrt{\mathrm{Re}}\right)}. \tag{4.4}$$

The validity of these formulas is a confirmation of the theoretical results summarized at the end of the theoretical part in points item 1 to item 3 and an answer to the questions posed there.
The good agreement between the measurements for naphthalene and those for liquids was cited above (subsection 3.2.1) as a reason why the liquid drops in the area examined can be treated like solid spheres when calculating evaporation. According to Equation 2.2 and figure 3.1 of my above-mentioned article [16], neglecting the effect of the liquid state, one obtains that in stationary falling motion the various Re values correspond to drops of the following sizes (at $\rho_1 = 1$), see Table 4.3.

Re stationary falling motion	1000	600	100	10	2	1
r, (mm)	1.07	0.79	0.30	0.105	0.058	0.042

Table 4.3: Values for r at Re numbers at stationary falling motion

4.1.3 Comparison with the Results of Takahasi

As mentioned in the introduction, Takahasi ([50], [51]) has published measurements of the evaporation of water droplets at $r = 0.2\,\mathrm{mm}$ to $1\,\mathrm{mm}$ and velocities of $1\,\mathrm{m\,s^{-1}}$ to $6\,\mathrm{m\,s^{-1}}$. He gave (with his notations) the formula

$$\left(\frac{\mathrm{d}r^2}{\mathrm{d}t}\right) = (0.45 + 0.078 \cdot v) \cdot \Delta b \cdot 10^{-4}\,, \tag{4.5}$$

where r is expressed in mm, t in s, v (velocity) in $\mathrm{m\,s^{-1}}$ and Δb in mm Hg. The quantity Δb is the difference between the absolute humidity and the saturation pressure at the air temperature. The formula, which was obtained purely empirically, contradicts the laws of similarity because according to them, Reynolds' number should appear in the brackets instead of v.
In Takahasi's experiments, the drops were suspended from glass threads and blown at from the side with airflow from an electric fan. To reduce turbulence, the air was only blown through funnel-shaped tubes. A vane anemometer was used to measure the air speed. The drops were repeatedly photographed, the square of their mean radius (r^2) was plotted as a function of time; A straight line was then obtained whose slope approximately followed Equation 4.5. Δb was 1 mm Hg to 9 mm Hg, the average variation $\pm 0.3 \times 10^{-4}\,\mathrm{mm^2\,s^{-1}}$.
My measurements give more accurate results for various reasons. According to control tests, the air flow had a good quality and its speed was measured almost at one point and without disturbance. However, the blowing from below in my case (see subsection 3.1.4) was more advantageous. In addition, there is the more precise measurement method (subsection 3.1.8), the measurability of the droplet temperature and the consideration of several sources of error. The r^2-t diagram is

not suitable for examining the dependence of evaporation on the droplet radius because the curve then appears to be straight. For example, if r^2 is reduced to a quarter, $\sqrt{r}$ is only reduced by a ratio of $1 : \sqrt{2}$, and the slope of the curve (see Equation 4.3) undergoes only a very small change. Using this method one gets $\left(\frac{\mathrm{d}r^2}{\mathrm{d}t}\right)$ for an average value of the radius.

The difference p between the vapor pressure values on the surface and in the air is decisive for evaporation. With a fairly good approximation, p was equal to the psychrometer vapor pressure difference (e.g. p'' mm Hg) (subsection 3.2.5), because the droplet temperature was usually only a few tenths of a degree above the temperature of the wet thermometer. Despite the different precision of the measurements, at least a qualitative agreement can be expected between my results and those of Takahasi. The proportionality between $\left(\frac{\mathrm{d}r^2}{\mathrm{d}t}\right)$ and Δb that he obtained should actually be between $\left(\frac{\mathrm{d}r^2}{\mathrm{d}t}\right)$ and p, i.e. approximately p''. However, this can also approximately apply to Δb, because $\frac{\Delta b}{p''}$ is constant in smaller areas with a rough approximation. For areas so small that the vapor pressure can be viewed as linearly dependent on temperature, this can easily be obtained from the usual psychrometer formula. If one sets the ratio $\frac{\Delta b}{p''} = 3$, one has to multiply the Takahasi values for $\left(\frac{\mathrm{d}r^2}{\mathrm{d}t}\right) \cdot \frac{1}{\Delta b}$ by approximately $4 \cdot 3$ in order to get corresponding results of my values for $\left(\frac{\mathrm{d}D^2}{\mathrm{d}t}\right) \cdot \frac{1}{p}$. Figure 4.8 contains the curves for $\left(\frac{\mathrm{d}D^2}{\mathrm{d}t}\right) \cdot \frac{1}{p}$ as a function of v calculated from my Equation 4.3. Different curves were obtained for the different drop sizes. According to my formula, the dashed area contains the values for the range of drop sizes and wind speeds examined by Takahasi. The figure also shows the Takahasi line. A qualitative match is obtained. The large spread of Takahasi's values is explained by these statements.

The deviations of Takahasi's formula from the laws of similarity are exactly the opposite of the deviations due to incomplete saturation on the surface (subsection 3.2.5). According to the facts stated above, Takahasi's results do not constitute a valid objection to my results.

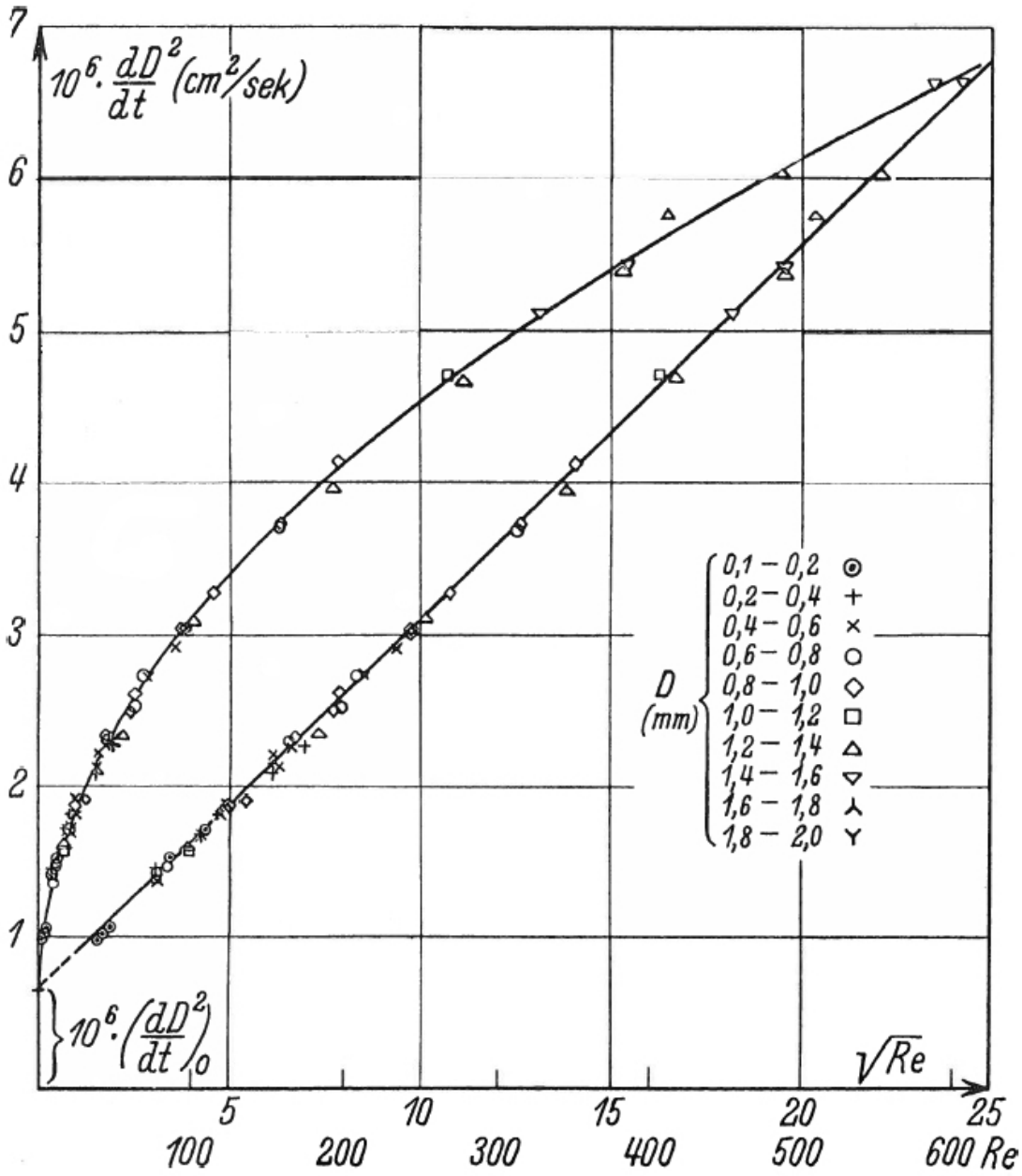

Figure 4.1: Measured evaporation $\frac{\mathrm{d}D^2}{\mathrm{d}t}$ or $\frac{\mathrm{d}D^2}{\mathrm{d}t} \cdot \frac{1}{p}$ for nitrobenzene as a function of $\sqrt{\mathrm{Re}}$

Re	$\sqrt{Re}$	$\frac{dD^2}{dt}$	Z	Re	$\sqrt{Re}$	$\frac{dD^2}{dt}$	Z	Re	$\sqrt{Re}$	$\frac{dD^2}{dt}$	Z
		$\cdot 10^{-6}$				$\cdot 10^{-6}$				$\cdot 10^{-6}$	
0	0	0.651		72.08	8.49	2.742	×	29.23	5.41	1.910	◇
24.55	4.95	1.838	◇	86.84	9.32	2.917	×	15.79	3.97	1.574	□
9.70	3.11	1.424	○	19.41	4.40	1.712	⊙	276.4	16.63	4.694	△
11.51	3.39	1.493	○	18.30	4.28	1.695	+	381.5	19.53	5.396	△
9.27	3.04	1.381	×	22.95	4.79	1.814	×	412.0	20.30	5.760	△
37.77	6.14	2.206	×	2.27	1.51	0.992	⊙	586.0	24.21	6.643	▽
24.72	4.97	1.900	×	42.95	6.55	2.299	○	383.8	19.59	5.441	▽
9.52	3.08	1.458	+	17.74	4.21	1.679	×	328.7	18.13	5.117	▽
114.7	10.71	3.256	◇	3.67	1.92	1.055	⊙	485.1	22.02	6.036	△
95.24	9.76	3.024	◇	9.40	3.06	1.381	○	197.1	14.04	4.134	◇
60.78	7.80	2.625	◇	2.93	1.71	1.019	⊙	267.1	16.34	4.724	□
42.77	6.54	2.263	×	38.63	6.22	2.136	×	157.4	12.54	3.718	○
11.54	3.40	1.522	⊙	48.5	6.96	2.264	+	192.4	13.87	3.956	△
36.36	6.03	2.080	+	158.5	12.59	3.735	◇	101.7	10.08	3.104	△
21.60	4.65	1.823	+	94.14	9.70	3.037	◇	52.75	7.26	2.352	△
62.15	7.88	2.524	○	45.23	6.72	2.311	◇	15.79	3.97	1.611	△
69.12	8.31	2.737	○	59.14	7.69	2.493	◇				

Figure 4.2: Measured values on which Figure 4.1 is based

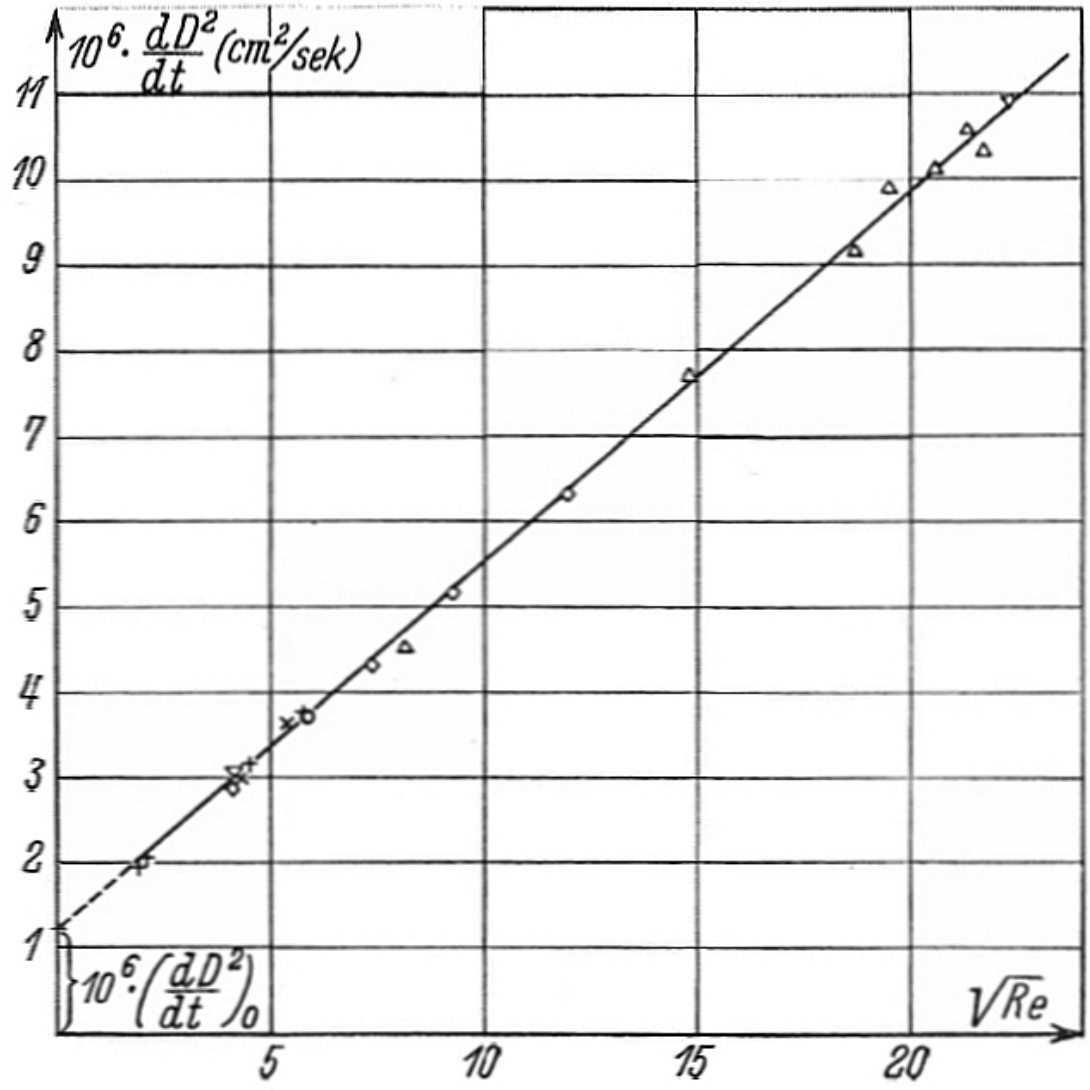

Figure 4.3: Measured evaporation $\frac{\mathrm{d}D^2}{\mathrm{d}t}$ or $\frac{\mathrm{d}D^2}{\mathrm{d}t} \cdot \frac{1}{p}$ for aniline as a function of $\sqrt{\mathrm{Re}}$

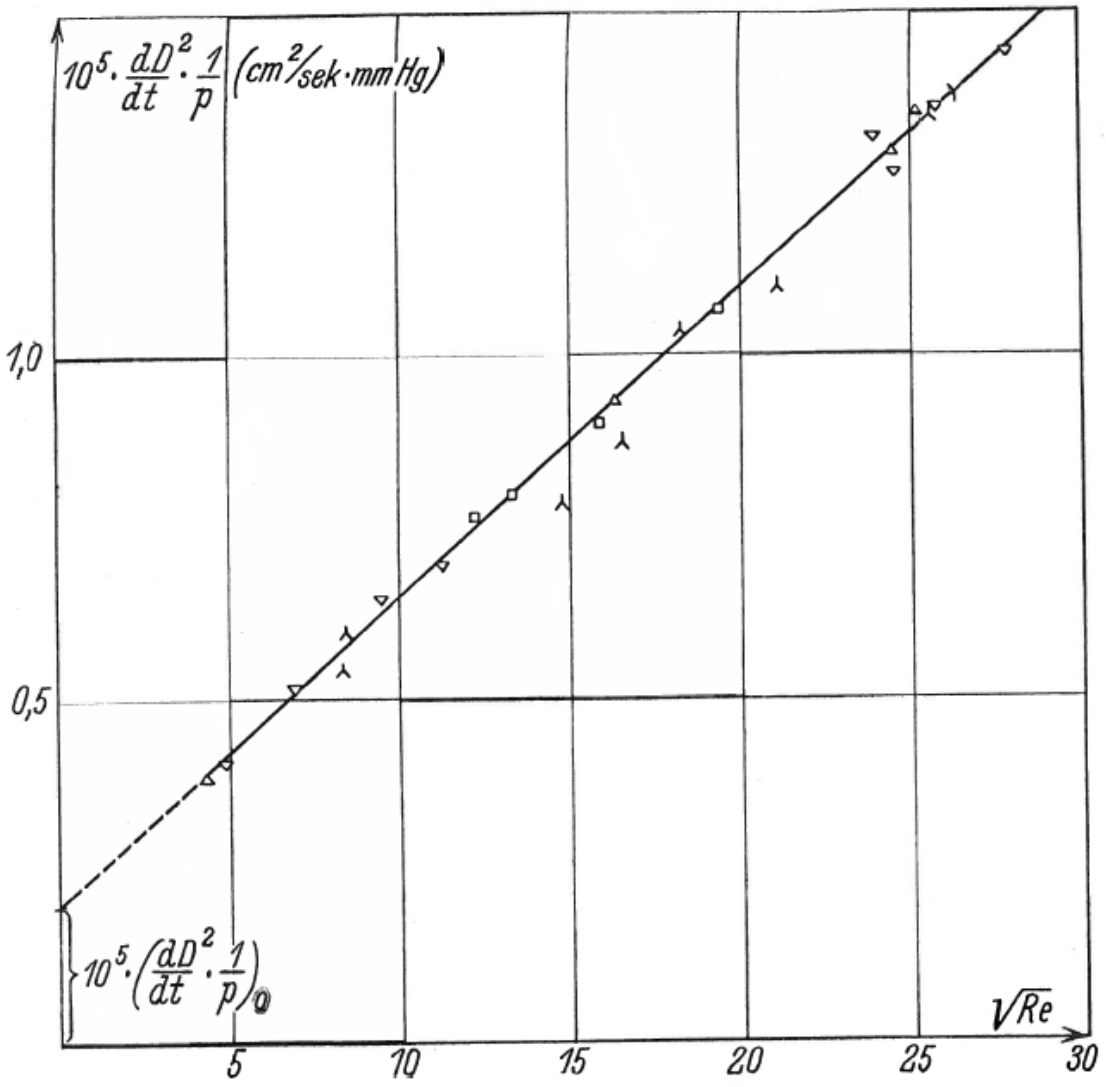

Figure 4.4: Measured evaporation $\frac{\mathrm{d}D^2}{\mathrm{d}t}$ or $\frac{\mathrm{d}D^2}{\mathrm{d}t} \cdot \frac{1}{p}$ for water as a function of $\sqrt{\mathrm{Re}}$

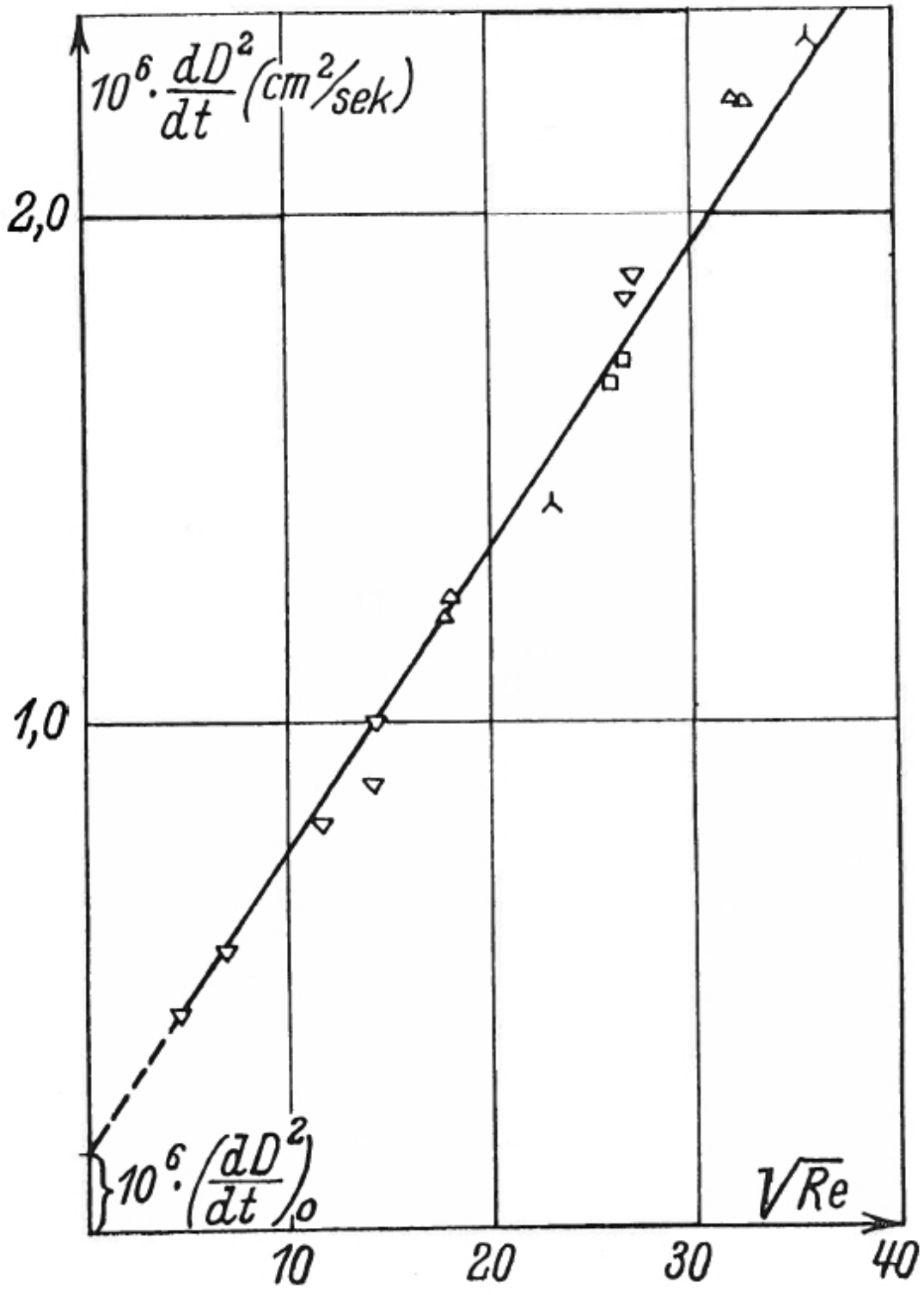

Figure 4.5: Measured evaporation $\frac{\mathrm{d}D^2}{\mathrm{d}t}$ or $\frac{\mathrm{d}D^2}{\mathrm{d}t} \cdot \frac{1}{p}$ for naphthalene as a function of $\sqrt{\mathrm{Re}}$

Fig. 4.3			Fig. 4.4			Fig. 4.5		
$\sqrt{Re}$	$\frac{dD^2}{dt}$	Z	$\sqrt{Re}$	$\frac{dD^2}{dt}\cdot\frac{1}{p}$	Z	$\sqrt{Re}$	$\frac{dD^2}{dt}$	Z
	$\cdot 10^{-6}$			$\cdot 10^{-5}$			$\cdot 10^{-6}$	
0	1.120		0	0.197		0	0.153	
8.18	4.542	△	12.16	0.763	□	26.48	1.710	□
5.85	3.735	○	13.30	0.797	□	25.95	1.659	□
4.30	3.002	×	11.20	0.693	▽	32.51	2.224	△
5.36	3.659	×	9.48	0.647	▽	32.00	2.234	△
9.25	5.179	◇	8.41	0.595	∧	18.00	1.246	△
4.47	3.167	+	8.28	0.544	∧	17.73	1.205	△
7.37	4.342	◇	6.92	0.517	▽	6.96	0.547	▽
11.91	6.319	◇	4.26	0.381	△	4.55	0.429	▽
5.76	3.766	+	4.86	0.405	▽	14.38	1.002	▽
4.16	2.858	◇	16.24	0.932	△	14.10	0.878	▽
1.92	1.961	+	15.93	0.899	□	11.68	0.800	▽
2.08	2.041	+	19.32	1.065	□	27.15	1.877	▽
4.18	3.079	▽	23.95	1.317	△	26.67	1.836	▽
19.43	9.889	△	25.57	1.348	∧	23.00	1.424	∧
18.67	9.139	△	24.55	1.264	▽	35.82	2.344	∧
21.37	10.58	△	24.49	1.296	△			
20.60	10.12	△	25.84	1.361	▽			
14.83	7.693	△	25.21	1.355	△			
22.35	10.90	▽	27.79	1.442	▽			
21.66	10.32	△	26.34	1.380	∨			
			21.07	1.096	∧			
			18.22	1.032	∧			
			16.54	0.872	∧			
			14.75	0.781	∧			

Figure 4.6: Measured values on which Figure 4.3, Figure 4.4 and Figure 4.5 are based

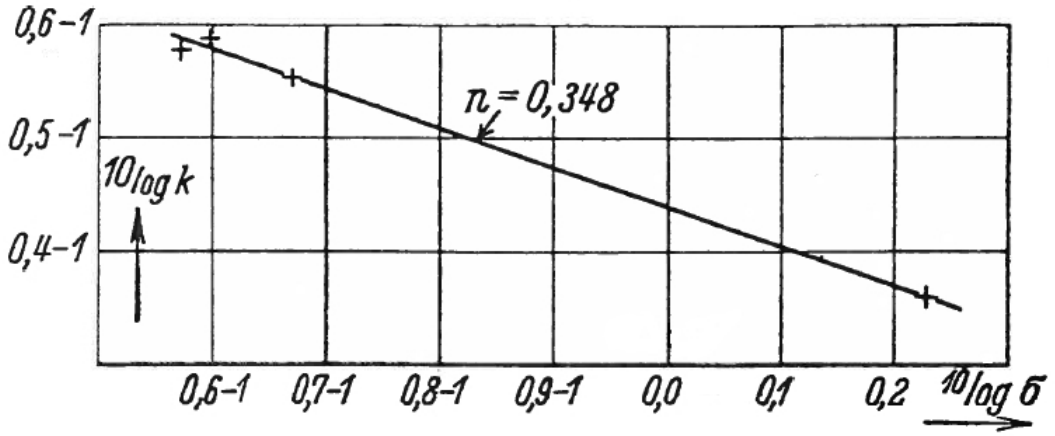

Figure 4.7: $\log(k)$ as a function of $\log(\sigma)$ for evaluation of the Ansatz $k = \frac{\text{const.}}{\sqrt[n]{\sigma}}$

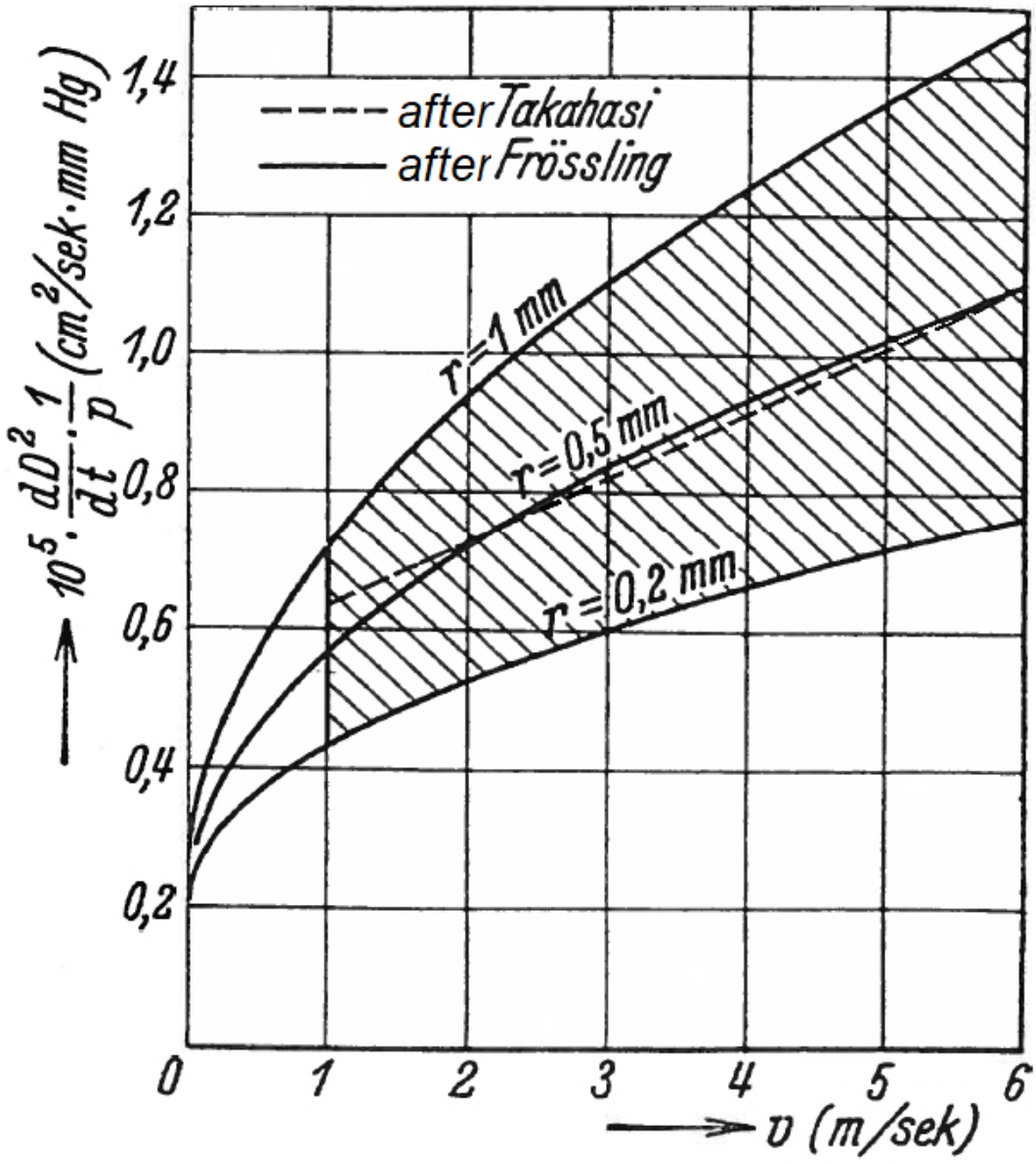

Figure 4.8: Curves for $\left(\frac{\mathrm{d}D^2}{\mathrm{d}t}\right) \cdot \frac{1}{p}$ as a function of v calculated from Equation 4.3

4.2 Measurement of the Evaporation Distribution

The distribution of evaporation over the surface was determined in the manner described in subsection 3.1.2 and subsection 3.1.8. Evaporation was reduced to 20 °C and 760 mm Hg and Nu′ was calculated from Equation 3.2. For different Re values, Nu′ was plotted as a function of the angle θ (calculated from the stagnation point) in Figure 4.9. Because of the unevenness of the surface, the scatter is quite large, but the points give a good qualitative picture of the distribution. Figure 3.2 (1 to 3) shows some images (Re = 0; 48; 1040 respectively). At no wind conditions, a uniform distribution is obtained, which was given in subsection 3.1.7 among the reasons for neglecting the convective wind. As an average value for some plates, Nu′ = 2 was obtained over the entire surface (as expected).
When the air moves, the distribution agrees with that which can be obtained from the flow patterns for the cylinder ([36]), where the flow is analogous. At Re < 1 the dead water begins to form and the evaporation on the rear side is much smaller than on the front. With larger Re numbers, the backflow and the oscillation in the wake become so strong that one can expect an increase in evaporation at the "rear stagnation point". This actually happened. A pronounced minimum emerged below the equator. The fact that the evaporation on the rear side was small was used above in the theoretical part. A source of error could arise from the fact that the naphthalene balls were displaced in the direction of the wind due to the pressure and as a result, evaporations that were too small were measured on the rear side. That this influence could have had only very little significance is evident from the following facts:

1. When photographing in the region of the equator section instead of the meridian section, whereby the bending of the glass thread was without any effect, the qualitatively same distribution occurred. In order to be able to examine the conditions in the "rear stagnation point", the meridian section that better corresponds to the spherical shape was photographed.

2. Using a magnifying glass, the shift when the wind begins to blow was observed on the screen used to adjust the camera. It was very small and disappeared when the flow was shielded (as in the exposed state).

Final words: The investigations were carried out in the Physics Institute of Lund University, and it is my pleasure to thank the director of the institute, Prof. Dr. J Koch, for providing me with a good place to work and for his willingness to provide me with the necessary apparatus.

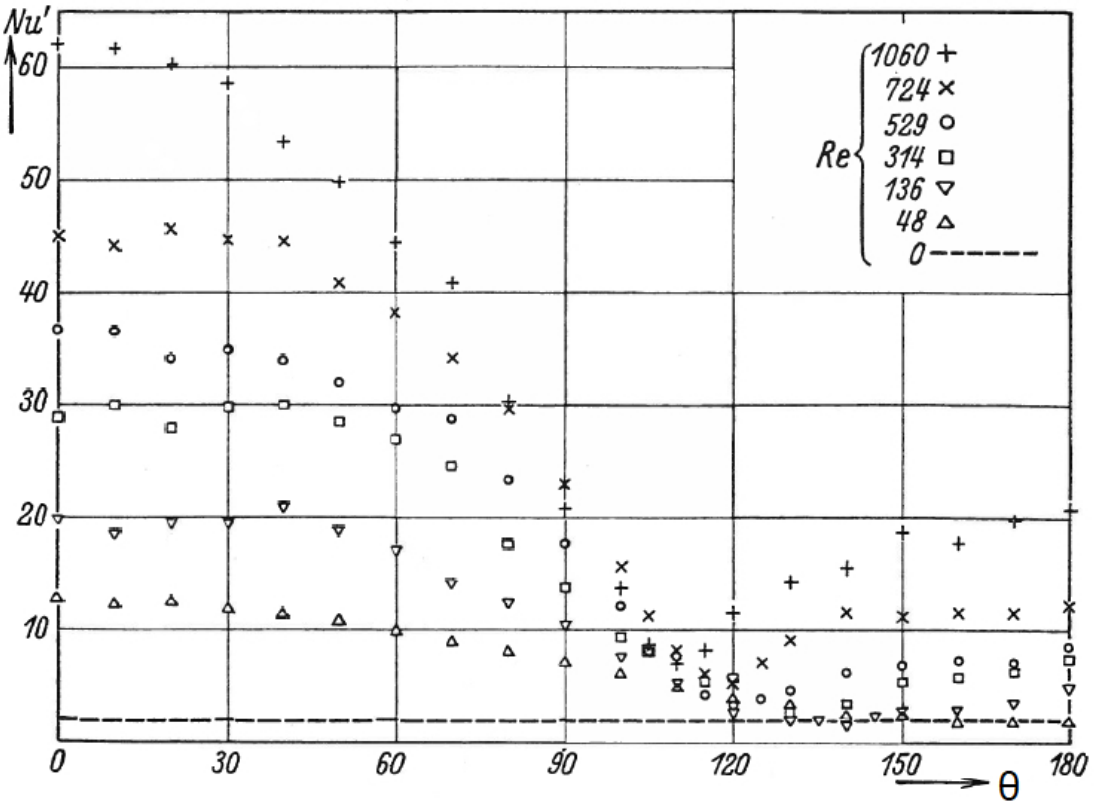

Figure 4.9: Nu′ plotted as a function of the angle θ (calculated from the stagnation point) for different Re values

Bibliography

[1] In H. H. Landolt and R. Börnstein, editors, *Physikalisch Chemische Tabellen*, volume 1 Erg.-Bd. Springer-Verlag, Berlin-Göttingen-Heidelberg, 1927. p. 806.

[2] In H. H. Landolt and R. Börnstein, editors, *Physikalisch Chemische Tabellen*, volume 2 Erg.-Bd. Springer-Verlag, Berlin-Göttingen-Heidelberg, 1931. p. 1280.

[3] In H. H. Landolt and R. Börnstein, editors, *Physikalisch Chemische Tabellen*, volume 3 Erg.-Bd. Springer-Verlag, Berlin-Göttingen-Heidelberg, 1936. p. 2462 – converted.

[4] In H. H. Landolt and R. Börnstein, editors, *Physikalisch Chemische Tabellen*, volume 3 Erg.-Bd. Springer-Verlag, Berlin-Göttingen-Heidelberg, 1936. p. 2462.

[5] In H. H. Landolt and R. Börnstein, editors, *Physikalisch Chemische Tabellen*, volume 3 Erg.-Bd. Springer-Verlag, Berlin-Göttingen-Heidelberg, 1936. p. 2421.

[6] F. Albrecht. Ein Meßgerät zur Messung und Registrierung kleiner Windgeschwindigkeiten und seine Anwendung auf die Untersuchung des Wärmeumsatzes an der Erdoberfläche. *Meteorologische Zeitschrift*, 47:465–474, 1930.

[7] T. Alty and C. A. MacKay. The accommodation coefficient and the evaporation coefficient of water. *Proceedings of the Royal Society of London. Series A - Mathematical and Physical Sciences*, 149(866):104–116, 1935.

[8] T. Alty and F. H. Nicoll. The Interchange of Molecules Between a Liquid and its Vapor. *Canadian Journal of Research*, 4(6):547–558, 1931.

[9] G. Bakker. Kapillarität und Oberflächenspannung. In W. Wien and F. Harms, editors, *Handbuch der Experimentalphysik*, volume 6. Akademische Verlagsgesellschaft, Leipzig, 1928. p. 184.

[10] R. Becker. *Theorie der Elektrizität, Bd. 1.* B.G. Teubner, 1933. p. 64.

[11] E. Boltze. *Grenzschichten an Rotationskörpern in Flüssigkeiten mit kleiner Reibung.* PhD thesis, Georg-August-Universität zu Göttingen, 1908.

[12] K. Büttner. Die Wärmeübertragung durch Leitung und Konvektion, Verdunstung und Strahlung in Bioklimatologie und Meteorologie. Technical Report 404, Königlich Preußisches Meteorologisches Institut, 1934.

[13] D. LeB. Cooper and E. P. Linton. A note on the use of hot wire anemometers. *Proceedings of the Nova Scotian Institute of Science*, 19(1):119–120, 1935.

[14] D. LeB. Cooper and E. P. Linton. Use of hot wire anemometers. *Physikalische Berichte*, 17:1097, 1936.

[15] O. Flachsbart. Neue Untersuchungen über den Luftwiderstand von Kugeln. *Physikalische Zeitschrift*, 28:461–469, 1927.

[16] N. Frössling. *Gerlands Beiträge zur Geophysik*, 51:167, 1937.

[17] N. Fuchs. Concerning the Velocity of Evaporation of small Droplets in a Gas Atmosphere. *Physikalische Zeitschrift der Sowjetunion*, 6:224–243, 1934.

[18] N. Gudris and L. Kulikowa. Die Verdampfung kleiner Wassertropfen. *Zeitschrift für Physik*, 25(1):121–132, 1924.

[19] H. G. Houghton. A Study of the Evaporation of Small Water Drops. *Physics*, 4:419–424, 1933.

[20] G Jäger. *Die Fortschritte der kinetischen Gastheorie*, volume 12 of *Die Wissenschaft*. Vieweg, Braunschweig, 2 edition, 1919.

[21] H. Jeffreys. Some problems of evaporation. *Philosophical Magazine*, 35(6):270–280, 1918.

[22] O. Krell. Druckverteilung an der luftumströmten Kugel. *Zeitschrift für Flugtechnik und Motorluftschiffahrt*, 22(4):97–105, 1931.

[23] G. Kroujiline. *Zentralblatt für Mechanik*, 4:430, 1936.

[24] G. Kroujiline. Investigation de la chouche-limite thermique. *Technical Physics of the U.S.S.R.*, 3:311–320, 1936.

[25] I. Langmuir. The Evaporation of Small Spheres. *Physical Review*, 12(5):368–370, 1918.

[26] S. Luthander and A. Ryberg. Experimentelle Untersuchungen über den Luftwiderstand bei einer um eine mit der Windrichtung Parallelen Achse rotieren Kugel. *Physikalische Zeitschrift*, 36:552–558, 1935. Fig. 5 und 6.

[27] S. Luthander and A. Ryberg. Experimentelle Untersuchungen über den Luftwiderstand bei einer um eine mit der Windrichtung Parallelen Achse rotieren Kugel. *Physikalische Zeitschrift*, 36:552–558, 1935. Fig. 12.

[28] H. Mache. Über die Verdunstungsgeschwindigkeit des Wasser in Wasserstoff und Luft. *Sitzungsberichte der mathematisch-naturwissenschaftlichen Classe der Kaiserlichen Akademie der Wissenschaften, Wien*, 2Abt-a-119:1399–1423, 1910.

[29] E. Jr. Mack. Average Cross-Sectional Areas of Molecules by Gaseous Diffusion Methods. *Journal of the American Chemical Society*, 47(10):2468–2482, 1925.

[30] H. W. Morse. On Evaporation from the Surface of a Solid Sphere. Preliminary Note. *Proceedings of the American Academy of Arts and Sciences*, 45(14):363–367, 1910.

[31] J. H. J. Müller and C. S. M. Pouillets. *Wärmelehre, Chemische Physik, Thermodynamik und Meteorologie*, volume 3 of *Lehrbuch der Physik und Meteorologie*. Braunschweig, Friedrich Vieweg und Sohn, 1926. p. 585.

[32] W. Nußelt. Das Grundgesetz des Wärmeübergangs. *Gesundheits-Ingenieur: Zeitschrift für die gesamte Städtehygiene*, 38:477–482, 490–496, 1915.

[33] W. Nußelt. Wärmeübergang, Diffusion und Verdunstung. *Zeitschrift für Angewandte Mathematik und Mechanik*, 10(2):105–121, 1930.

[34] W. Paeschke. Feuchtigkeitseffekt bei Hitzdrahtmessungen. *Physikalische Zeitschrift*, 36:564–565, 1935.

[35] E. Pohlhausen. Der Wärmeaustausch zwischen festen Körpern und Flüssigkeiten mit kleiner reibung und kleiner Wärmeleitung. *Zeitschrift für Angewandte Mathematik und Mechanik*, 1(2):115–121, 1921.

[36] L. Prandtl and O. Tietjens. *Hydro- und Aeromechanik. Bd. II.* Berlin, Julius Springer, 1 edition, 1931. Figure 3, 4 und 23.

[37] Roller. *Praktische Schulphysik*, 15:166–169, 1935.

[38] L. Schiller. 1. Teil: Hydro- und Aerodynamik. In W. Wien and F. Harms, editors, *Handbuch der Experimentalphysik*, volume 4. Akademische Verlagsgesellschaft, Leipzig, 1931. p. 239.

[39] L. Schiller. 1. Teil: Hydro- und Aerodynamik. In W. Wien and F. Harms, editors, *Handbuch der Experimentalphysik*, volume 4. Akademische Verlagsgesellschaft, Leipzig, 1931. p. 285.

[40] L. Schiller. 1. Teil: Hydro- und Aerodynamik. In W. Wien and F. Harms, editors, *Handbuch der Experimentalphysik*, volume 4. Akademische Verlagsgesellschaft, Leipzig, 1931. p. 279.

[41] L. Schiller. 1. Teil: Hydro- und Aerodynamik. In W. Wien and F. Harms, editors, *Handbuch der Experimentalphysik*, volume 4. Akademische Verlagsgesellschaft, Leipzig, 1931. p. 639, Equation 4b.

[42] L. Schiller. 1. Teil: Hydro- und Aerodynamik. In W. Wien and F. Harms, editors, *Handbuch der Experimentalphysik*, volume 4. Akademische Verlagsgesellschaft, Leipzig, 1931. p. 113.

[43] Schreber. *Beiträge zur Physik der freien Atmosphäre*, 12:215, 1925.

[44] G. B. Schubauer. Effect of Humidity on Hot-Wire Anemometry. *Journal of Research of the National Bureau of Standards*, 15:575–578, 1935.

[45] M. Smulochowski. Drei Vorträge uber Diffusion. Brownsche Bewegung und Koagulation von Kolloidteilchen. *Physikalische Zeitschrift*, 17:557–585, 1916.

[46] Sresnewski. *Journal der russischen physikalisch-chemischen Gesellschaft*, 14:420, 1882.

[47] J. Stefan. Über die dynamische Theorie der Diffusion der Gase. *Sitzungsberichte der mathematisch-naturwissenschaftlichen Classe der Kaiserlichen Akademie der Wissenschaften, Wien*, 2Abt-65:323–363, 1872.

[48] J. Stefan. Versuche über die Verdampfung. *Sitzungsberichte der mathematisch-naturwissenschaftlichen Classe der Kaiserlichen Akademie der Wissenschaften, Wien*, 2Abt-68:385–423, 1873.

[49] J. Stefan. Über die Verdampfung aus einem kreisförmig oder elliptisch begrenzten Becken. *Sitzungsberichte der mathematisch-naturwissenschaftlichen Classe der Kaiserlichen Akademie der Wissenschaften, Wien*, 2Abt-83:943–954, 1881.

[50] Y. Takahashi. Über die experimentelle Versuchung von Wassertropfenverdunstung und einige Anwenduugen auf die Regentropfen. *Journal of the Meteorological Society of Japan*, 13(7):302–311, 1935.

[51] Y. Takahashi. *Geophysical Magazine*, 10:321, 1936.

[52] B. Topley and Whytlaw-Gray R. Experiments on the rate of evaporation of small spheres as a method of determining diffusion coefficients.– The diffusion coefficient of iodine. *Philosophical Magazine*, 4(24):873–888, 1927.

[53] E. W. Washburn. *International Critical Tables of Numerical Data, Physics, Chemistry and Technology*, volume 3.

[54] E. W. Washburn. *International Critical Tables of Numerical Data, Physics, Chemistry and Technology*, volume 5.